Coordination Chemistry Reviews 256 (2012) 1229–1245

Contents lists available at SciVerse ScienceDirect

Coordination Chemistry Reviews

journal homepage: www.elsevier.com/locate/ccr

Review

Bioinspired functional mimics of the manganese catalases

Sandra Signorella[a,*], Christelle Hureau[b,c]

[a] Facultad de Ciencias Bioquímicas y Farmacéuticas, Universidad Nacional de Rosario, IQUIR (Instituto de Química Rosario) – CONICET, Suipacha 531, S2002LRK Rosario, Argentina
[b] CNRS, LCC (Laboratoire de Chimie de Coordination), 205, route de Narbonne, F-31077 Toulouse, France
[c] Université de Toulouse, UPS, INPT, LCC, F-31077 Toulouse, France

Contents

ARTICLE INFO

Article history:
Received 29 October 2011
Accepted 6 February 2012
Available online 16 February 2012

Keywords:
Manganese
Catalases
Bioinorganic chemistry
Structure–activity
Redox

ABSTRACT

Catalase enzymes are present in most aerobic forms of life and are responsible for the decomposition of hydrogen peroxide to molecular oxygen and water. Although most catalases contain the iron-protoporphyrin IX prosthetic group, some bacteria utilize a non-heme manganese containing catalase (MnCAT). The active site of these enzymes contains two Mn ions triply bridged by a $\mu_{1,3}$-carboxylato from a Glu residue and two solvent-derived single atom bridges. Determination of their exact catalytic mechanism is precluded by their fast kinetics. Hence biomimetic compounds may help providing valuable insights into the mechanisms of these enzymes. Indeed, comparison of the activity of structurally characterized complexes can help delineating the functional roles of the bridging ligands and structural motifs that play a key function in H_2O_2 disproportionation. Moreover, due to the potential use as catalytic scavengers of H_2O_2 for preventing oxidative stress injuries, numerous and diverse Mn compounds have been reported to have CAT-like activity. The present review is focused on non-porphyrinic mimics of MnCAT. Several families of Mn-based catalysts are described, the properties of which are commented on, stressing the role of bridging and terminal ligands on redox potentials and catalysis.

* Corresponding author at: Facultad de Ciencias Bioquímicas y Farmacéuticas, Universidad Nacional de Rosario, IQUIR (Instituto de Química Rosario) – CONICET, Suipacha 531, S2002LRK Rosario, Argentina.
E-mail address: signorella@iquir-conicet.gov.ar (S. Signorella).

0010-8545/$ – see front matter © 2012 Elsevier B.V. All rights reserved.
doi:10.1016/j.ccr.2012.02.003

Nomenclature

benzimpnOH *N*,*N*,*N*′,*N*′-tetrakis(2-methylenebenzimidazolyl)-1,3-diaminopropan-2-ol
bimindH 1,3-bis(2′-benzimidazolylimino)isoindoline
bipy 2,2′-bipyridine
bispicMe$_2$en *N*,*N*′-bis[(2-pyridylmethyl)(methyl)]-1,2-ethanediamine
HPClNOL 1-[bis-(2-pyridylmethyl)amino]-3-chloropropan-2-ol
bpbpmp 2-[bis(2-pyridylmethyl)aminomethyl]-6-{[(benzyl)(2-pyridylmethyl)amino]methyl}-4-methylphenol
bpea *N*,*N*-bis(2-methylpyridyl)ethylamine
bpeaph *N1*,*N1*′-(1,3-phenylenebis(methylene)bis(*N2*,*N2*′-bis(pyridine-2-ylmethyl)ethane-1,2-diamine)
bpemp 2,6-bis{bis(2-(2-pyridylethyl)amino)methyl}-4-methylphenol
bpep 2,6-bis{bis(2-(2-pyridylethyl)amino)methyl}phenol
bphpmp 2-[bis(2-pyridylmethyl)aminomethyl]-6-{[(2-hydroxybenzyl)(2-pyridylmethyl)amino]methyl}-4-methylphenol
bpia bis(picolyl)(*N*-methylimidazol-2-yl)amine
bpmapa bis((2-pyridylmethyl)amino)propionic acid
bpmp 2,6-bis{(*N*,*N*-bis(2-pyridylmethyl)amino)methyl}-4-methylphenol
bphba 2-{(*N*,*N*-bis(2-pyridylmethyl)amino)methyl}phenol
chedam 4-hydroxypyridine-2,6,dicarboxylic acid
cyclam 1,4,8,11-tetraazacyclotetradecane
cyclam$_2$^{i}PrOH 1,3-bis[1,4,8,11-tetraazacyclotetradecane]propan-2-ol
dmaiBrp 4-bromo-2-{[(dimethylamino)ethyl]iminomethyl}-6-{[(dimethylamino)ethyl](methyl)aminomethyl}phenol
dmamp 2,6-bis{[(dimethylamino)ethyl]aminomethyl}-4-methylphenol
dmimp 2,6-bis{[(dimethylamino)ethyl]iminomethyl}-4-methylphenol
dpimp 2,6-bis{(2-pyridylmethyl)iminomethyl}-4-methylphenol
Hbbml [bis(2-benzimidazolylmethyl)amino]ethanol
Hbpg bis(2-picolyl)glycylamine
H$_3$bprol-^{t}Bu-p 2,6-bis(prolin-1-yl)methyl-4-t-butylphenol
Hetsalim ethyl salicylimidate
H$_3$nta nitrilo-tris-acetic acid
H$_2$pda 2-picolyldiglycylamine
hpmp 2,6-bis{((2-hydroxybenzyl)(2-pyridylmethyl)amino)methyl}-4-methylphenol
hppentOH 1,5-bis[(2-hydroxybenzyl)(2-pyridylmethyl)amino]pentan-3-ol
hppnOH 1,3-bis[(2-hydroxybenzyl)(2-pyridylmethyl)amino]propan-2-ol
indH 1,3-bis(2′-pyridylimino)isoindoline
LH *N*,*N*-bis(2-pyridylmethyl)-*N*′-(salicylidene)ethane-1,2-diamine
L^{i}H *N*-(2-hydroxybenzyl)-*N*-(2-pyridylmethyl)-*N*′-(2-pyridylmethyliminato)ethane-1,2-diamine
mLH *N*,*N*′-bis(2-pyridylmethyl)-*N*-(2-hydroxybenzyl)-*N*′-methylethane-1,2-diamine
pbpmapa α-phenyl-β-[bis(2-pyridylmethyl)amino]propionic acid
phen 1,10-phenanthroline
pmpemp 2,6-bis{[2-(2-pyridyl)ethyl(2-pyridylmethyl)amino]methyl}-4-methylphenol
salen 1,2-bis(salicylideneamino)ethane
salbutOH 1,4-bis(salicylideneamino)butan-2-ol
salpentOH 1,5-bis(salicylideneamino)pentan-3-ol
salpn 1,3-bis(salicylideneamino)propane
salpnOH 1,3-bis(salicylideneamino)propan-2-ol
tacn 1,4,7-triazacyclononane
tpa tris-2-picolylamine = tris(2-methylpyridyl)amine

Abbreviations
CAT catalase
EPR electron paramagnetic resonance
ESI-MS electrospray ionization mass spectrometry
FAB-MS fast atom bombardment mass spectrometry
GSH glutathione
SOD superoxide dismutase
SCE saturated calomel electrode
NHE normal hydrogen electrode

1. Introductory remarks

Reactive Oxygen Species (ROS) are generated in the respiratory chain by successive reductions of dioxygen to superoxide radical and hydrogen peroxide (Scheme 1) [1–3]. While H_2O_2 is not a strong oxidant by itself, it can form the highly reactive hydroxyl radical by Fenton-like reactions in the presence of metallic traces. In general, concentrations of these species are tightly controlled since they are useful in several biological events as apoptosis or redox signaling; but increased levels of ROS have been observed in several pathologies, including ischemia, reperfusion-related injuries and neurodegenerative diseases [4–7]. Superoxide dismutases (SOD), catalases (CAT) and the glutathione (GSH) peroxidase are the enzymes involved in defense against oxidative stress. Two CAT families exist. The most abundant CAT contain a iron(III)-protoporphyrin prosthetic group [8]. In the other family, the active site is made of a dinuclear Mn core (MnCAT) [9,10]. The present review is focused on functional mimics of the MnCAT and thus on non-porphyrinic complexes. A number of families of Mn-based catalysts that employ different oxidation states during catalysis are described, the properties of which are commented on, stressing the role of bridging and terminal ligands on redox potentials and catalysis.

2. Manganese catalase

Catalase enzymes are present in most aerobic forms of life and are responsible for the decomposition of hydrogen peroxide to molecular oxygen and water [11,12]. Although most catalases contain the iron-protoporphyrin IX prostetic group, some bacteria utilize a non-heme Mn containing catalase [13–16]. Two crystal structures at atomic resolution have been obtained for MnCAT isolated from *Lactobacillus plantarum* [10] and *Thermus thermophilus* [9,17]. The active site of these enzymes contains two Mn ions triply bridged by a $\mu_{1,3}$-carboxylato from a Glu residue and two solvent-derived single atom bridges, the exact nature of which is yet to be established. In the Mn_2^{III} form of *L. plantarum* and *T. thermophilus*, the Mn···Mn separation is 3.03 [10] and 3.14 Å [9], respectively. EPR and EXAFS studies have suggested that the Mn···Mn separation is significantly longer in the reduced Mn_2^{II} form of the enzyme (3.53 Å), consistent with water and/or hydroxide as the bridging oxygen atoms [18,19]. Furthermore, the Mn2 subsite is coordinated to one His and one bidentate carboxylate from a Glu residue. The Mn1 subsite is bound to one His and one monodentate Glu carboxylate, with the sixth coordination site occupied by a terminal

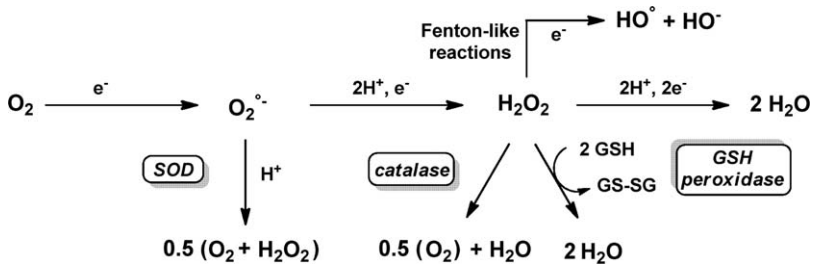

Scheme 1. Simplified view of the oxygen reduction route showing the enzymes involved in ROS detoxification.

water molecule in octahedral coordination geometry (Fig. 1). Terminally bound water molecules are easily displaced from the metal complexes and this apical site likely serves as the initial substrate binding site during catalysis [20].

Dismutation of H_2O_2 by MnCAT shows saturation kinetics on substrate, described by the Michaelis–Menten model depicted in Scheme 2.

According to this model, initial rates (r_i) vs. $[H_2O_2]_i$ plots can be fitted to Eq. (1), the Michaelis–Menten equation.

$$r_i = \frac{k_{cat}[MnCAT][H_2O_2]_i}{K_M + [H_2O_2]_i} = \frac{V_{max}[H_2O_2]_i}{K_M + [H_2O_2]_i} \quad (1)$$

In this equation, k_{cat} is the catalytic rate constant (also known as turnover number), K_M ($k_{-1}k_{cat}/k_1$) is a measure of the enzyme affinity for H_2O_2 (the lower the K_M value, the higher the affinity for H_2O_2) and V_{max} is the maximal rate attained for a given enzyme concentration. For MnCAT, the turnover-limiting step (the slow step in the catalytic cycle associated to k_{cat}) is the reduction of H_2O_2 [21]. Turnover numbers of 2.6×10^4, 2.6×10^5 and 2×10^5 s^{-1} and K_M 15, 83 and 350 mM were reported for MnCAT from *Thermoleophilum album* [22,23], *T. thermophilus* [21] and *L. plantarum* [22], respectively. Turnover numbers of MnCAT, although quite fast, are significantly slower than those of heme-CAT that are close to the diffusion-limited rate.

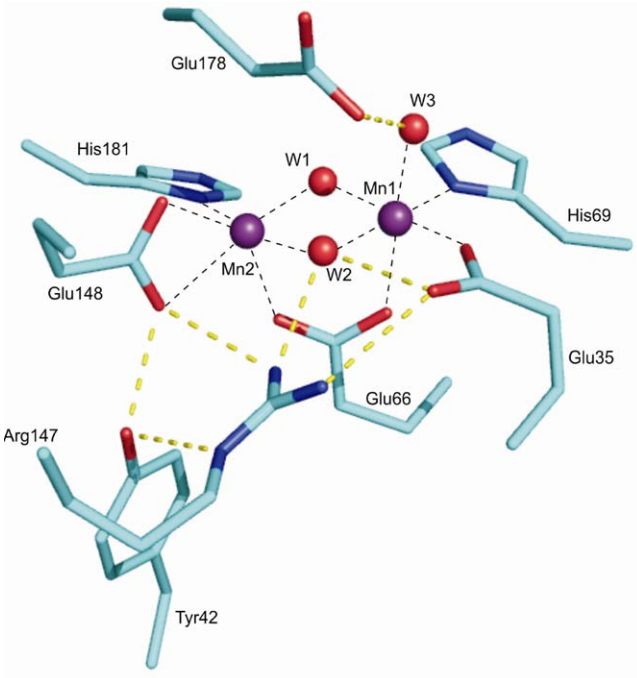

Fig. 1. Active site of dimanganese catalase from *L. plantarum* (adapted from PDB ID 1JKU).

$$MnCAT + H_2O_2 \underset{k_{-1}}{\overset{k_1}{\rightleftharpoons}} MnCAT\text{-}H_2O_2 \xrightarrow{k_{cat}} MnCAT + Product$$

Scheme 2. Michaelis–Menten model.

Although MnCATs have been isolated in four oxidation states ranging from Mn_2^{II} to $Mn_2^{III,IV}$, biochemical and spectroscopic studies have shown that these enzymes disproportionate H_2O_2 by cycling between the Mn_2^{II} and Mn_2^{III} oxidation states [24,25]. Hence, removal of the catalytically inactive mixed valence $Mn_2^{II,III}$ and $Mn_2^{III,IV}$ states may be crucial in high efficient enzymatic CAT activity. At pH 7, the electrochemical potentials (vs. NHE: normal hydrogen electrode) for the two-electron O_2/H_2O_2 and H_2O_2/H_2O couples are +0.28 and +1.35 V, respectively. To efficiently catalyze the H_2O_2 disproportionation, the protein environment controls the reduction potential of the dimanganese active site to a value much lower than that of the Mn^{3+}/Mn^{2+} couple (1.54 V). The fact that the two Mn ions of the active site of MnCAT possess the same NO_5 coordination sphere provides a symmetrical environment that stabilizes the homovalent diMn core and facilitates the observed redox activity based on shuttling between Mn_2^{II}/Mn_2^{III} states during disproportionation of H_2O_2. Also, carboxylato bridges electronically shield the diMn center, thus promoting two-electron Mn_2^{II}/Mn_2^{III} over one-electron $Mn_2^{II}/Mn_2^{II,III}/Mn_2^{III}$ processes [11].

Because of the fast kinetics of this enzymatic reaction, each independent step of the catalytic cycle of MnCATs has not yet been characterized. However, based on reactivity, structural and spectroscopic studies of MnCAT and derivatives, a mechanism for the H_2O_2 disproportionation by MnCAT (shown in Scheme 3) has been proposed involving distinct coordination modes for peroxide substrate in each of the two oxidation states of the enzyme during turnover [26].

In this mechanism, oxidation state changes are accompanied by structural changes involving the groups binding the Mn atoms. Initial peroxide binding to the Mn_2^{III} form of the enzyme occurs at a terminal site on one of the Mn centers by displacement of the labile water ligand with concomitant protonation of the μ-oxo bridge, followed by reduction of the dimanganese center and release of O_2. The second equivalent of H_2O_2 binds to the Mn_2^{II} form of the enzyme as a bridging $\mu_{1,1}$-hydroperoxo, protonation of which facilitates heterolytic O—O bond cleavage coupled to cluster reoxidation with loss of water, closing the catalytic cycle. Terminal and bridging peroxide binding to the Mn_2^{III} and Mn_2^{II} forms of the enzyme, respectively, are supported by X-ray studies of the azide and halide inhibited enzyme: azide binds to the oxidized Mn_2^{III} state of the enzyme as a terminal ligand [10] and halides bind the reduced Mn_2^{II} state replacing the μ-oxygen bridges by the μ-chloride ones [9,25].

In MnCAT, a web of hydrogen bonds contributes to stabilize the diMn core with the pair of solvent bridges, making MnCAT active over a wide pH range of 5–12, with activity nearly independent of pH in the 7–10 pH range, and falling to zero at more extreme pH values [27–29]. The loss of catalytic activity at pH < 5 was attributed to protonation of the bridges and formation of an

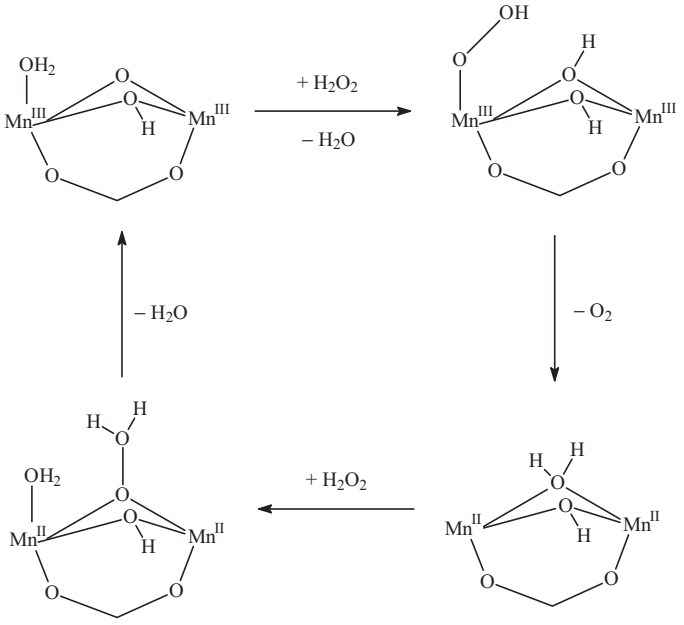

Scheme 3. Mechanism of catalytic disproportionation of H_2O_2 by MnCAT adapted from Ref. [26].

open form of the enzyme, thus supporting that the active site of the enzyme must contain a closed cluster mediated by a pair of solvent bridges [20].

3. Manganese catalase mimics

Biomimetic compounds provide a unique way for testing mechanisms in MnCAT enzymes. Comparison of the activity of structurally characterized complexes can help delineating the functional roles of the bridging ligands and structural motifs that play a key role in the mechanism of H_2O_2 disproportionation by these enzymes. In particular, the fine-tuning of Mn redox states appears as a critical feature when using artificial compounds to mimic the enzymatic activity. A challenge of bioinorganic chemistry is to rationalize the involvement of the Mn_2^{II}/Mn_2^{III}, $Mn_2^{II,III}/Mn_2^{III,IV}$ or Mn_2^{III}/Mn_2^{IV} couples in the H_2O_2 disproportionation catalyzed by diMn complexes on the basis of structural differences of the Mn_2 centers provided by the ligands.

Due to the potential use as catalytic scavengers of H_2O_2 for preventing oxidative stress injuries, numerous and diverse Mn compounds exhibiting CAT-like activity have been reported [12]. However, more detailed mechanistic studies have been performed on complexes of binucleating ligands involving either alkoxo or phenolato which provide an internal bridge to stabilize the dimanganese unit. In this review, the relevant features of these functional mimics and their CAT activity are presented and some insights into the role of the bridging ligands, endogenous bases, and first- and second-sphere effects on the redox potentials and catalysis are discussed. These systems will be compared to diMn complexes with N/O ancillary ligands and different bridging motifs, with regard to redox properties and catalase activity. Effect of water on complexes with exchangeable ligands and implications on their CAT activity will be illustrated with some chosen examples. Drawn structures of complexes discussed in this review are based on reported crystal structures, unless otherwise mentioned. The various ligands to which references will be made are summarized in Scheme 4.

4. Alkoxo-bridged diMn catalysts

Dinucleating diamine and diimine, which provide one alkoxo oxygen for the endogenous bridging of two metal ions, have been employed with success in the synthesis of functional mimics for MnCAT [30–38]. Kinetic and mechanistic studies of the H_2O_2 disproportionation by these complexes have revealed some structural features that control the Mn oxidation states involved in the catalase activity. Four alkoxo-bridged diMn systems disproportionate H_2O_2 with saturation kinetics, through a redox cycle involving the $Mn^{III}{}_2/Mn^{II}{}_2$ couple [30–38]. These complexes contain polydentate ligands derived from 1,3-diaminopropan-2-ol or 1,5-diaminopentan-3-ol, that modulate the Mn···Mn separation to 3.2–3.3 Å and 2.95 Å, respectively, and possess $Mn^{III}{}_2(\mu\text{-OR})_2{}^{4+}$ [33,34], $Mn^{II}{}_2(\mu\text{-OAc})(\mu\text{-OR})(H_2O)^{2+}$ [32,36], $Mn^{III}{}_2(\mu\text{-OAc})_2(\mu\text{-OR})^{3+}$ [37] or $Mn^{III}{}_2(\mu\text{-OAc})(\mu\text{-OR})_2{}^{3+}$ [30,37] cores with the remaining coordination sites of the two Mn ions occupied by donor atoms of the ligand (Fig. 2). These compounds have been proposed to undergo alkoxide-shift [38], carboxylate-shift [30,37] (that is the replacement of the coordinated ligand by the substrate) or possess one labile position [31,35], thus offering a terminal coordination site to H_2O_2. For complexes of X-hppentOH and benzimpnOH, ESI-MS, UV–vis, EPR and paramagnetic ^{1}H NMR spectroscopies demonstrated that the starting compounds undergo methoxo (or water)/oxo exchange in basic medium, with retention of bound acetato either as a bridge or shifted to a terminal position. Based on spectroscopic results, the oxo-bridged complexes, $[Mn^{III}{}_2(\mu\text{-O})(\mu\text{-AcO})(\text{X-hppentO})]$ and $[Mn_2{}^{III}(\mu\text{-O})(\text{OAc})(\text{OH})(\text{benzimpnO})]^+$ [30,31] were proposed as the active forms of the catalysts during H_2O_2 disproportionation. A striking point that results from comparison of these systems concerns the turnover-limiting step. For X-hppentOH, X-hppnOH and X-salpnOH systems the rate determining step of the cycle corresponds to reduction of the catalyst with simultaneous oxidation of H_2O_2 (oxidative half-reaction), with endogenous ligands acting as internal bases facilitating deprotonation of peroxide during its oxidation, in agreement with the fact that the rate is not affected by addition of an external base.

However, for the benzimpnOH complex, the oxidation of the $Mn_2{}^{II}$ complex to the oxo-bridged-$Mn_2{}^{III}$ form with concomitant reduction of H_2O_2 (reductive half-reaction) occurs in the slow step of the catalytic cycle [31]. This fact was explained by the higher redox potential of the Mn^{II}/Mn^{III} couple in $[Mn_2{}^{II}(\mu\text{-OAc})(\mu\text{-OH}_2)(\text{benzimpnO})]^{2+}$ with respect to the other alkoxo-bridged complexes (Table 1, entries 1–5), which is a consequence of the increased N/O ratio in the coordination sphere of Mn (N_3O_3 vs. N_2O_4 or NO_5). A similar behavior was exhibited by $[Mn_2{}^{II}(\text{cyclam}_2{}^{i}\text{PrOH})(\mu\text{-O}_3\text{SCF}_3)]^{2+}$, a robust complex with Mn in a N_4O_2 coordination sphere with high stability of the $Mn_2{}^{II}$ oxidation state (Table 1, entry 6), and that disproportionates 20,000 equivalents of H_2O_2 [39]. Another interesting observation is that complexes $[Mn_2{}^{III}(\mu\text{-OAc})(\mu\text{-OMe})(\text{X-hppentO})]^+$ are stable over a ≈1 V potential range [30] while $[Mn_2(\mu\text{-OAc})(\mu\text{-OMe})(\text{hppnO})]^+$ and $[Mn^{III}(\text{X-salpnO})]_2$ are stable in a narrower ΔE range (≈0.6 V), and the $Mn^{III}{}_2/Mn^{III}Mn^{IV}$ couple is shifted to significantly lower potentials, as shown for $[Mn_2{}^{III}(\mu\text{-OAc})(\mu\text{-OMe})(\text{hppnO})]^+$ in Fig. 3(a). This figure illustrates cyclic voltammograms of the $Mn^{III}{}_2/Mn^{III}Mn^{IV}$ couple taken at different scan rates [37]. The increased stability of the $diMn^{III}$ oxidation state was interpreted as the result of the increase in the chelate ring size provided by the length of the linkers between the central alcohol and the N-amino groups of the ligands (see Section 5.1 for other examples) [40,41].

These four classes of complexes disproportionate H_2O_2 with saturation kinetics (entries 1–4 of Table 2), with similar k_{cat} values but significantly higher than k_{cat} obtained for complexes possessing $Mn_2(\mu\text{-OAc})_2{}^{2+}$ or $Mn_2(\mu\text{-OPh})_2{}^{2+(\text{or } 4+)}$ cores

($0.02–0.2\ s^{-1}$) [43] (entries 7–9, Table 2). In every case, k_{cat} and K_M values were obtained from non-linear fit of experimental data to the Michaelis–Menten equation (solid lines in Fig. 4 are good examples of this kind of fit). K_M values in Table 2 also reflect the relative affinity of the alkoxo-bridged catalysts for the substrate: complexes with one labile position > complexes undergoing alkoxide-shift > complexes undergoing carboxylate-shift.

X-salpentOH yields another family of alkoxo-bridged diMn complexes (Fig. 5) that employ the Mn^{III}_2/Mn^{IV}_2 couple to dismutate H_2O_2 [42,44–47]. Complexes of this family contain polydentate Schiff-base ligands derived from 1,5-diaminopentan-3-ol that modulate the intermetallic distance to 2.91–2.94 Å, possess a $Mn^{III}_2(\mu\text{-OAc})(\mu\text{-OR})_2^{3+}$ core with two labile coordination sites in *cis*-position to each other and dismutate H_2O_2 with saturation kinetics (entry 5 in Table 2).

BINUCLEATING LIGANDS

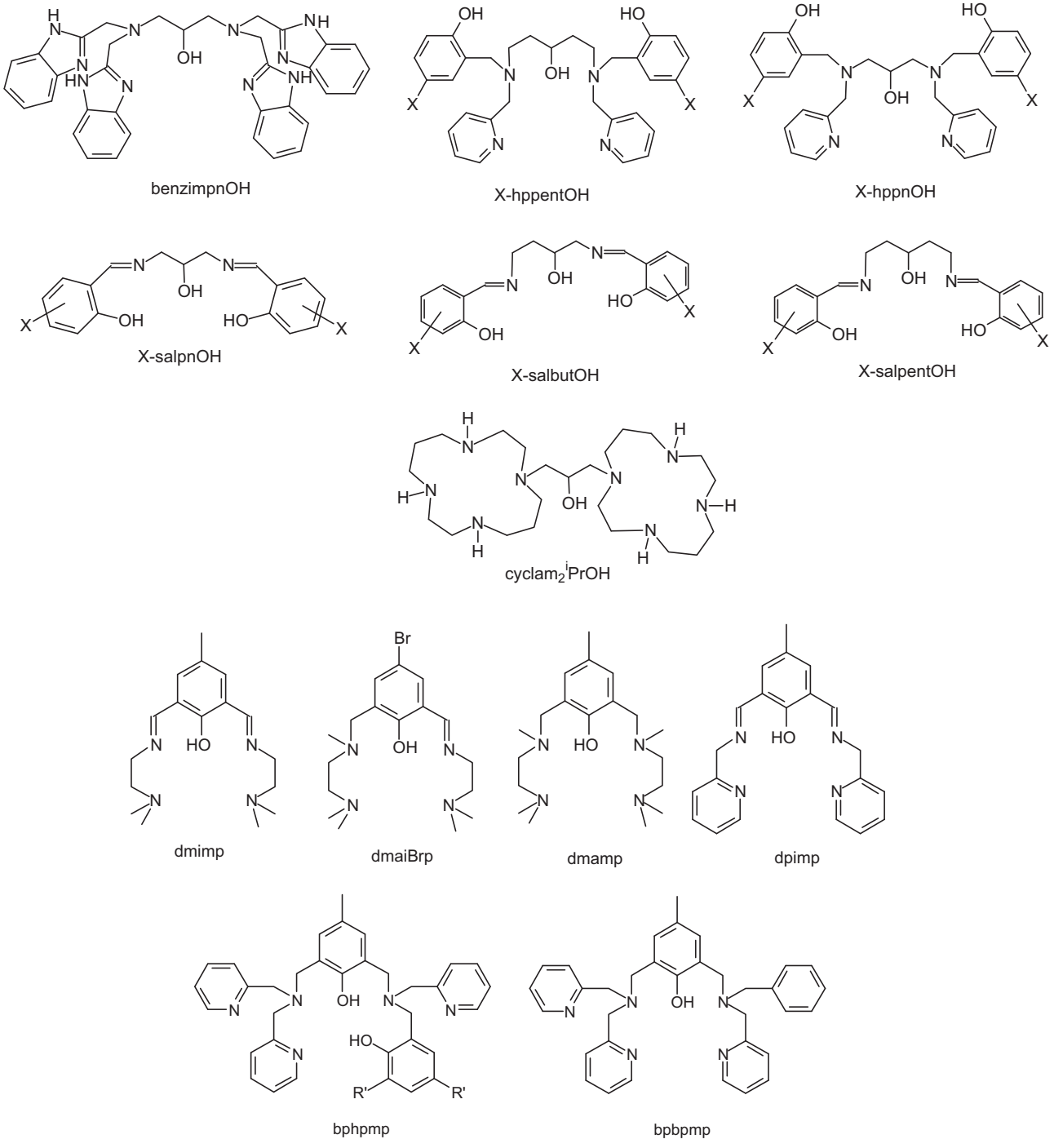

Scheme 4. Ligands and their abbreviations.

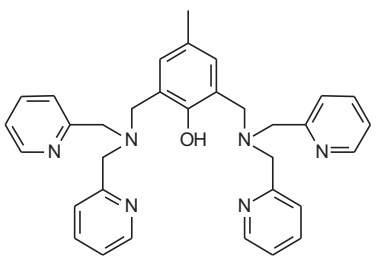

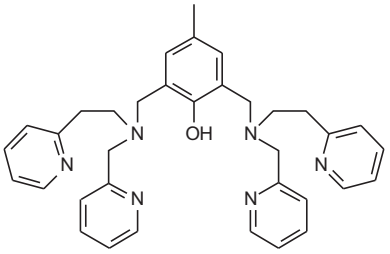

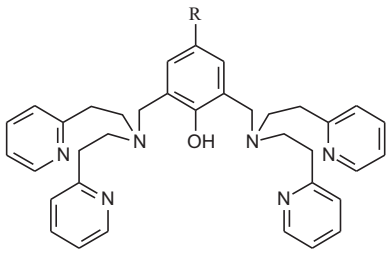

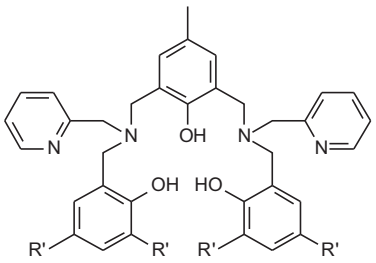

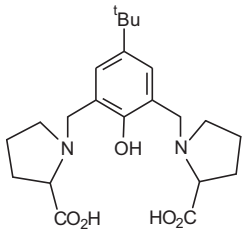

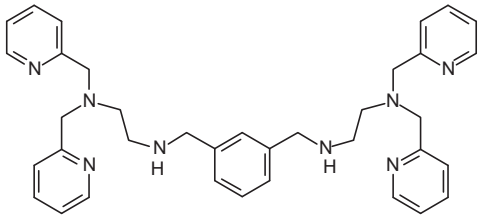

NON-BINUBLEATING LIGANDS

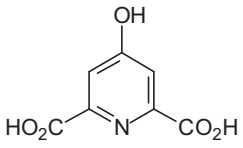

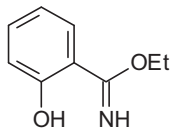

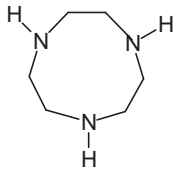

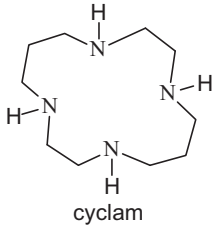

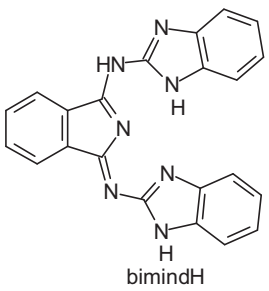

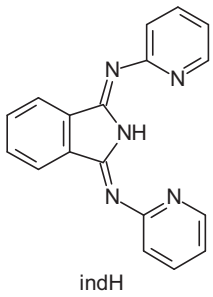

Scheme 4. (*Continued*)

Kinetic studies of H_2O_2 disproportionation catalyzed by Mn_2^{III} complexes of X-salpentOH showed that the catalysts that are easier to oxidise react faster (electron-donating > H > electron withdrawing substituent). The complex with X = 3-OMe reacted faster than expected from its redox potential, a fact attributed to the contribution of the *ortho*-OMe group in the deprotonation of H_2O_2, activating it toward O—O bond cleavage [42]. Although the redox potentials of complexes of X-salpentOH (entry 5 in Table 1, and Fig. 3(b)) fall in the same range as those of complexes of X-salpnOH or X-hppnOH, the H_2O_2 disproportionation cycle involves interconversion between the Mn^{III}_2 and $[Mn^{IV}{=}O]_2$ forms. Both the short Mn···Mn separation and the occurrence

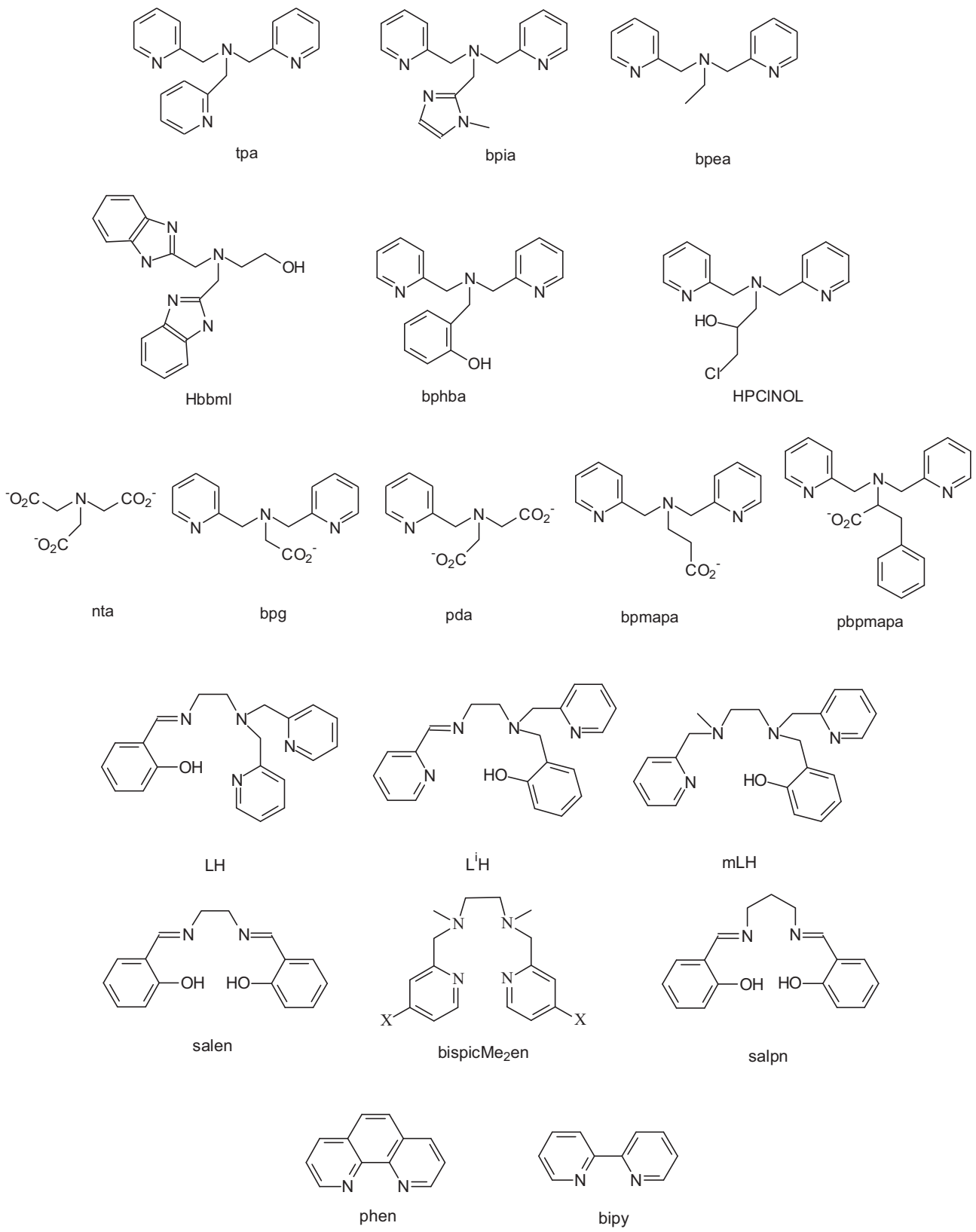

Scheme 4. (*Continued*)

of two labile coordination sites has been thought to facilitate the μ-bridging mode of peroxide leading to O—O cleavage and formation of the $[Mn^{IV}{=}O]_2$ form of catalyst. This should not be the case for complexes of X-hppentOH because, despite the short Mn···Mn distance (2.95 Å), saturation of the coordination sphere of the Mn ions by non-labile donors enforces peroxide to bind Mn as a terminal ligand (through ligand-shift). X-salpnOH and benzimpnOH mimics combine long intermetallic distance and none (or one) labile site on the Mn ions, thus favoring terminal binding of peroxide. In line with these facts, and although no

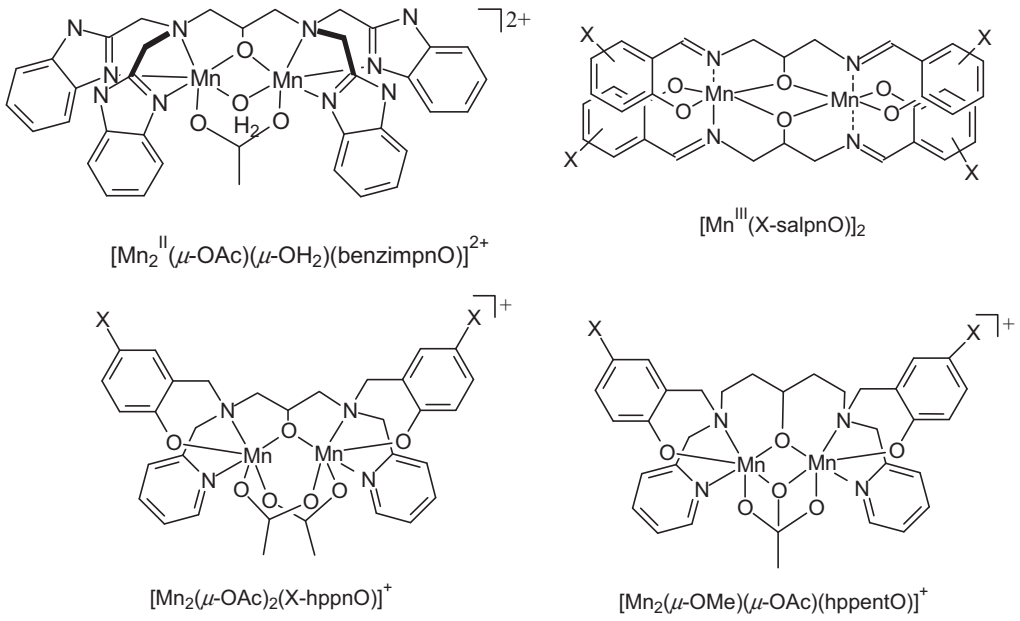

Fig. 2. Alkoxo-bridged diMn complexes that employ the Mn_2^{II}/Mn_2^{III} cycle to disproportionate H_2O_2.

Table 1
Redox potentials (vs. SCE) of alkoxo- and oxo-bridged diMn complexes.

	Complex	$Mn_2^{III,II}/Mn_2^{II}$	$Mn_2^{III}/Mn_2^{III,II}$	$Mn_2^{III,IV}/Mn_2^{III}$	$Mn_2^{IV}/Mn_2^{III,IV}$	Solvent	Donor set around Mn	Mn–Mn distance	Ref.
1	$[Mn^{III}(X^1\text{-salpnO})]_2$		−0.37 to 0.11	0.2–0.7		CH_3CN	N_2O_4	3.25	[33]
2	$[Mn_2^{II}(\mu\text{-OAc})(\mu\text{-OH}_2)(\text{benzimpnO})]^{2+}$		0.79[b]	1.25		CH_3CN	N_3O_3	3.54	[32]
3	$[Mn_2^{III}(\mu\text{-OAc})(\mu\text{-Y})(X^2\text{-hppnO})]^+$		−0.5 to −0.2[a]	0.19–0.34		CH_3CN	N_2O_4	3.2	[37]
4	$[Mn_2^{III}(\mu\text{-OAc})(\mu\text{-OMe})(X^3\text{-hppentO})]^+$		−0.13 to 0.03	>1		DMF	N_2O_4	2.95	[30]
5	$[Mn_2^{III}(\mu\text{-OAc})(\mu\text{-OMe})(X^4\text{-salpentO})(MeOH)_2]^+$		−0.19 to 0.1	0.31–0.61		DMF	NO_5	2.91–2.94	[42,44–47]
6	$[Mn_2^{II}(\text{cyclam}_2{}^i\text{PrO})(\mu\text{-O}_3SCF_3)]^{2+}$	0.79	1.1	1.5		CH_3CN	N_4O_2	3.844	[39]
7	$[(OAc)Mn^{III}(bbml)_2Mn^{III}(OAc)]^{2+}$		−0.45[a,c]	0.55[a]	0.85[a]	DMF	N_3O_3	3.21	[48]
8	$[Mn_2^{III,IV}(\mu\text{-O})_2(tpa)_2]^{3+}$			0.25	1.17	CH_3CN	N_4O_2	2.643	[96]
9	$[Mn_2^{III,IV}(\mu\text{-O})_2(bpg)_2]^+$			−0.04	0.73	CH_3CN	N_3O_3	2.66	[96]
10	$[Mn_2^{III,IV}(\mu\text{-O})_2(pda)_2]^-$			−0.06	0.67	CH_3CN/H_2O	N_2O_4	–	[96]
11	$[Mn_2^{III,IV}(\mu\text{-O})_2(X^5\text{-bispicMe}_2\text{en})_2]^{3+}$			0.1–0.3	0.97–1.32	CH_3CN	N_4O_2	2.678	[100,101]

[a] Irreversible.
[b] Bielectronic redox couple.
[c] Tentative assignment.
Y = OAc or OMe. X = aromatic ring substituents: X^1 = 5-OCH_3, H, 5-Cl, 3,5-diCl, 5-NO_2; X^2 = OMe, H, Cl; X^3 = OMe, H, Br; X^4 = OMe, Me, H, Cl, Br, NO_2; X^5 = H, OEt, Me, Cl, NO_2.

mechanistic studies have been performed, a Mn_2^{II}/Mn_2^{III} redox cycle can be expected for $[(OAc)Mn^{III}(bbml)_2Mn^{III}(OAc)]^{2+}$, a complex with a $Mn^{III}{}_2(\mu\text{-OR})_2{}^{4+}$ core, Mn···Mn distance of 3.21 Å and two terminal acetato *trans* to each other, which disproportionates H_2O_2 in acetonitrile:H_2O solution with initial turnover rate of 0.858 s^{-1} in the presence of imidazol [48].

5. Phenoxo-bridged diMn complexes

5.1. Electrochemical properties

Dinucleating ligands which provide one phenoxo oxygen for the endogenous bridging of two metal ions, and two arms with polydentate chelating donor sets have proved to maintain the integrity of the dinuclear center through variable oxidation states [49–54]. It has been observed that the aromatic ring connecting the chelating arms provide a rigid spacer for a bridged dinuclear complex that confers an entropic advantage in concerted reactions of the two metal ions with the substrate [55]. A comparison of the electrochemical behavior of these phenoxo-bridged complexes illustrate some of the chemical implications of first- and second-sphere effects on the redox properties of the metal centers that are relevant to the fine-tuning of Mn redox states of functional mimics.

5.1.1. Nature of the donor set around the Mn ion

Among dinuclear Mn complexes bridged by phenoxo oxygen atoms, the donor set around each Mn ion has a major effect in modulating the Mn oxidation state. An increase of the O/N ratio in the first-coordination sphere stabilizes Mn in higher valence state. Thus, the negative charge of the three phenolate groups in $[Mn_2(^t\text{Bu-hpmp})(\mu\text{-OAc})_2]^+$ [52,53] results in significant stabilization of the higher oxidation states of the Mn ions compared to $[Mn^{II}{}_2(bpmp)(\mu\text{-OAc})_2]^+$ (Fig. 6) that has only one bridging phenoxo group of the bpmp ligand (Table 3, entries 1 and 5) [49,50].

The potentials for the $Mn_2^{III}/Mn_2^{II,III}$ and $Mn_2^{II,III}/Mn_2^{II}$ couples of $[Mn_2(^t\text{Bu-hpmp})(\mu\text{-OAc})_2]^+$ are lowered by 0.8 and 1 V compared with $[Mn_2(bpmp)(\mu\text{-OAc})_2]^+$ and a third metal centered oxidation attributable to the $Mn_2^{III}/Mn_2^{III,IV}$ couple is also observed

Table 2
Kinetic parameters for catalyzed H_2O_2 disproportionation.

	Catalyst	k_{cat} (s^{-1})	K_M (mM)	Solvent, T (°C)	Ref.
DiMn catalysts that disproportionate H_2O_2 with saturation kinetics[a]					
1	$[Mn_2(\mu\text{-OAc})_2(X^1\text{-hppnO})]^+$	3.4–23	150–600	DMF, 25	[37]
2	$[Mn_2(\mu\text{-OMe})(OAc)(X^2\text{-hppentO})]^+$	1.31–2.8	88–170	DMF, 10	[30]
3	$[Mn(X^3\text{-salpnO})]_2$	4.2–21.9	10–120	CH_3CN, 25	[38]
4	$[Mn_2(\mu\text{-O})(OAc)(OH)(benzimpnO)]^+$	2.7	6	MeOH:H_2O, 25	[31]
5	$[Mn_2(\mu\text{-OMe})(\mu\text{-OAc})(X^4\text{-salpentO})S_2]^+$	0.75–7.9	16–78	DMF, 25	[42,44–47]
6	$Mn_2^{II,III}(\mu\text{-OAc})_2(bphpmp)]^+$	2.48	83[b]	NR, 25	[64]
7	$[Mn_2(X^5\text{-bphba})_2Cl_2]$	0.017–0.075	20–151	H_2O, 25	[65]
8	$[Mn^{III}_2(etsalim)_4(Hetsalim)_2]^{2+}$ + 5 equiv. OH^-	0.038	21	EtOH, 25	[86]
9	$[Mn^{II}(bpia)(\mu\text{-OAc})]_2^{2+}$	0.237	45	DMF, 25	[90]
10	$[Mn_2^{III,IV}(\mu\text{-O})_2(\mu\text{-OAc})(Me_3\text{-tacn})(OAc)_2]$	5.5[c]	–	Acetate buffer (pH 4.6), 20	[98]
11	$[Mn_2^{III,IV}(\mu\text{-O})_2(\mu\text{-OAc})(Me_3\text{-tacn})(bipy)]^{2+}$	13.2[c]	–	Acetate buffer (pH 4.6), 20	[98]
12	$[Mn^{II}_2(\mu\text{-Cl})_2tpa_2]^{2+}$	107	3100	CH_3CN, 25	[102]
13	$[Mn^{IV}(\mu\text{-O})(salpn)]_2$	250	250	Cl_2CH_2/CH_3CN, 25	[105,106]

	Catalyst	k_{cat} ($M^{-1}\,s^{-1}$)	Solvent, T (°C)	Ref.
DiMn catalysts that disproportionate H_2O_2 with second order kinetics[d]				
14	$[Mn_2^{II}(bprol\text{-}^tBu\text{-}p)(\mu\text{-OAc})(H_2O)_2]^{2+}$	0.29	DMF, 20	[72]
15	$[Mn_2^{II,III}(bpbpmp)(\mu\text{-OAc})_2(H_2O)]^{2+}$	14.5[e]	CH_3CN, 0	[77]
16	$[Mn_2^{III,IV}(\mu\text{-O})_2(tpa)_2]^{3+}$	0.065[e]	CH_3CN, 0	[96]
17	$[Mn_2^{III,IV}(\mu\text{-O})_2(bpg)_2]^+$	0.29[e]	CH_3CN, 0	[96]
18	$[Mn_2^{III,IV}(\mu\text{-O})_2(pda)_2]^-$	1.6[e]	CH_3CN, 0	[96]
19	$[Mn_2^{III,IV}(\mu\text{-O})_2(X^6\text{-bispicMe}_2en)_2]^{3+}$	14–35[e]	Phosphate buffer (pH 7.5–8), 30	[100]

NR, not reported.
[a] Saturation kinetics: rates described by the Michaelis–Menten model.
[b] mmol.
[c] V_{max}/[cat].
[d] Second order kinetics: $r_i = k_{cat}$ [catalyst] [H_2O_2].
[e] Values estimated from reported rate data.
S = solvent. X = aromatic ring substituents: X^1 = OMe, Cl; X^2 = OMe, H, Br; X^3 = 5-OCH_3, H, 5-Cl, 3,5-diCl, or 5-NO_2; X^4 = OMe, Me, H, Cl, Br, NO_2; X^5 = OMe, Me, H, NO_2; X^6 = H, OEt, Me, Cl, NO_2.

Table 3
Redox potentials vs. SCE of phenolato-bridged diMn complexes, in CH_3CN.

	Complex	$Mn_2^{II}/Mn_2^{II,III}$	$Mn_2^{II,III}/Mn_2^{III}$	$Mn_2^{III}/Mn_2^{III,IV}$	Mn coordination sphere	Ref.
1	$[Mn_2^{II}(bpmp)(\mu\text{-OAc})_2]^+$	0.47	1.03	1.75[a]	N_3O_3	[49,50]
2	$[Mn_2^{II}(pmpemp)(\mu\text{-OAc})_2]^+$	0.59	1.2	–	N_3O_3	[60]
3	$[Mn_2^{II}(bpemp)(\mu\text{-OAc})_2]^+$	0.65	1.22[a]	–	N_3O_3	[63]
4	$[Mn_2^{II}(bpep)(\mu\text{-OAc})_2]^+$	0.73	1.3[a]	–	N_3O_3	[59]
5	$[Mn_2^{III}(^tBu\text{-hpmp})(\mu\text{-OAc})_2]^+$	−0.32	0.04	0.95	N_2O_4	[52,53]
6	$[Mn_2^{II,III}(bp\text{-}^tBu\text{-hpmp})(\mu\text{-OAc})_2]^+$	−0.21	0.6	0.97	N_3O_3, N_2O_4	[51]
7	$[Mn_2^{II,III}(bphpmp)(\mu\text{-OAc})_2]^+$	−0.23	0.74	–	N_3O_3, N_2O_4	[64]
8	$[Mn_2^{II}(X\text{-bphba})_2Cl_2]$[b]	0.43–0.75[c]	–	–	N_3O_2Cl	[65]
9	$[Mn_2^{II}(bpbpmp)(\mu\text{-OBz})_2(H_2O)]^+$	0.51	1.28[a]	–	$N_3O_3/N_2O_3O_w$	[78]
10	$[Mn_2^{II,III}(bpbpmp)(\mu\text{-OAc})_2(H_2O)]^{2+}$	0.45	1.18[a]	–	$N_3O_3/N_2O_3O_w$	[78]

[a] Irreversible.
[b] bis(phenolato)-bridged.
[c] CH_3CN/DMF. X = OMe, Me, H, NO_2.

below 1 V [52,53]. The nature of the N-donor group also modulates the stability of a given oxidation state of the Mn ion in phenoxo-bridged diMn complexes. This is illustrated by LH and L^iH (Fig. 7), which afford Mn_2^{II} complexes with the $Mn_2^{II}(\mu\text{-OPh})_2^{2+}$ core that can be oxidized to the Mn_2^{III} complex at 0.46 [56] and 0.58 V [57] (vs. SCE, CH_3CN), respectively, without alteration of the dinuclear structure. The imine/phenolato or imine/pyridine fragments in these complexes stabilizes the high oxidation states of the metal and the oxidation to the Mn_2^{III} complex occurs at potential about 0.5 V lower than for other diphenoxo bridged Mn_2^{II} complexes with amine/phenolato fragments (i.e. $[Mn_2^{II}(mL)_2]^{2+}$, 0.89 V [58]).

5.1.2. Size of the metallacycle

The chelate ring size is another factor to limit the stability of the oxidation states in dinuclear Mn complexes. This effect is illustrated by the dinucleating ligands bpmp, bpemp and pmpemp, which differ in their chelate arm lengths (Fig. 6). While bpmp and pmpemp afford Mn_2^{II} and $Mn_2^{II,III}$ in stable forms [49,59,60], bpemp only yields complex in the Mn_2^{II} state in a stable form [61–63]. These stabilities were rationalized by the difference in the coordination geometry and radii requirements of the Mn^{II} and Mn^{III} ions. Chelating ligands that preclude short bonds or impose rigid distortion to the octahedral geometry angles, destabilize the Mn^{III} state with respect to reduction. Therefore, the redox potentials increase with the chelate ring sizes of the ligand in the order bpmp < pmpemp < bpemp (Fig. 6, Table 3, entries 1–3).

5.1.3. Nature of the substituent on phenolato ligand(s)

For a number of phenolato-bridged dinuclear Mn complexes it has been established that the redox potentials are decreased by inductive effects of electron-donating substituents on the phenolato ring with a linear correlation of the Hammett constant σ_p and the redox potential. The introduction of a *p*-methyl substituent on the phenolato ring causes the decrease of the redox potentials of the $Mn_2^{II}/Mn_2^{II,III}$ and $Mn_2^{II,III}/Mn_2^{III}$ couples of $[Mn_2(bpemp)(\mu\text{-OAc})_2]^+$ by 0.08 V relative to those of $[Mn_2(bpep)(\mu\text{-OAc})_2]^+$ (Table 3, entries 3 and 4) [59,63]. Introduction of *tert*-butyl

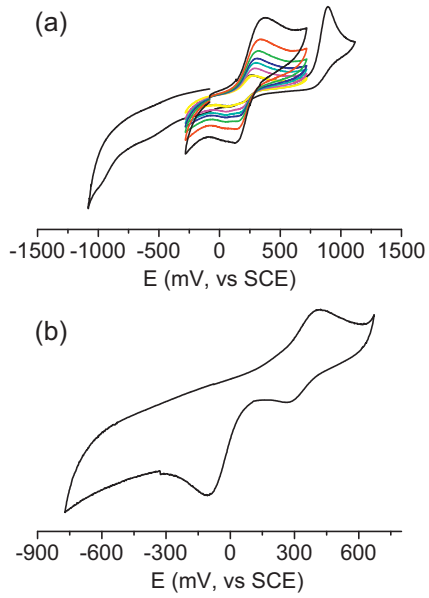

Fig. 3. Cyclic voltammograms of (a) $[Mn_2^{III}(\mu\text{-OAc})(\mu\text{-OMe})(hppnO)]^+$ in CH_3CN: scan rates = 100–2000 mV/s (shown in different colors); (b) $[Mn_2^{III}(\mu\text{-OAc})(\mu\text{-OMe})(5\text{-Me-salpentO})]^+$ in DMF: scan rate = 100 mV/s.
Adapted from Refs. [37,42].

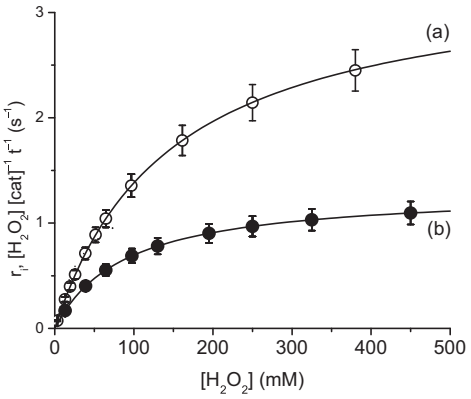

Fig. 4. Fit of initial rate values to the Michaelis–Menten equation for (a) $[Mn_2(\mu\text{-OAc})_2(5\text{-OMe-hppnO})]^+$ and (b) $[Mn_2^{III}(\mu\text{-OAc})(\mu\text{-OMe})(5\text{-OMe-hppentO})]^+$, in DMF. Vertical bars: standard deviation from at least 5 independent experiments.
Adapted from Refs. [30,37].

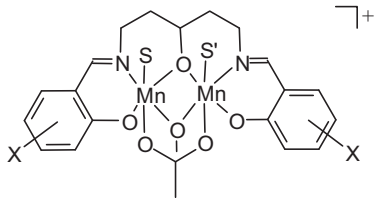

$[Mn_2(\mu\text{-OMe})(\mu\text{-OAc})(X\text{-salpentO})SS']^+$

Fig. 5. Alkoxo-bridged diMn complexes that employ the Mn_2^{III}/Mn_2^{IV} redox cycle to dismutate H_2O_2.

substituents on terminal phenol rings results in a decrease of 0.14 V in the $Mn_2^{II,III}/Mn_2^{III}$ couple (Table 3, entries 6 and 7) [51,64]. The redox potentials of complexes with the $Mn_2^{II}(\mu\text{-OPh})_2^{2+}$ core also correlate with the insertion of electron-withdrawing or -donating substituents (redox potentials increase from OMe to NO_2, Table 3, entry 8) [65].

5.1.4. Water content and formation of μ-oxo species

Charge accumulation in oxidation processes performed in non-aqueous solvents precludes the formation of stable oxidation states beyond the Mn_2^{III} one. Electrochemical, EPR and XAS investigations on $[Mn_2^{II}(bpmp)(\mu\text{-OAc})_2]^+$ and $[Mn_2^{III}(^t\text{Bu-hpmp})(\mu\text{-OAc})_2]^+$ have shown that the presence of water induces changes in the coordination mode between the two Mn ions that facilitates the redox transition to yield $[Mn_2^{III}(bpmp)(\mu\text{-OAc})(\mu\text{-O})]^{2+}$ and $[Mn_2^{III,IV}(^t\text{Bu-hpmp})(\mu\text{-OAc})(\mu\text{-O})]^+$ at potential <1 V [66]. Thus, higher oxidation states can be accessed at much lower potentials than in the absence of water due to the formation of μ-oxo bridged species. The oxidation potential at which this the water insertion occurs depends on the N/O ratio in the coordination sphere of the Mn ions and on the water content [51,67]. For $[Mn_2^{II}(bpmp)(\mu\text{-OAc})_2]^+$, when the water content is high, exchange of the acetato bridges by water derived ligands is favored for the lower oxidation states and the potential required for the formation of di-μ-oxo-bridged $Mn^{III}Mn^{IV}$ dimers drops below the potential of the $Mn_2^{II,III}/Mn_2^{III}$ of the di-acetato complex [67]. Similarly, for $[Mn_2^{III}(^t\text{Bu-hpmp})(\mu\text{-OAc})_2]^+$, the presence of water enhances the stability of the $Mn^{III}Mn^{IV}$ state and leads oxidation to occur at lower potentials to yield $[Mn_2^{III,IV}(^t\text{Bu-hpmp})(\mu\text{-O})]^+$ or even bis-oxido-$Mn_2^{III,IV}$ species [53].

5.2. Symmetrical MnCAT mimics

A number of pentadentate phenol-based dinucleating ligands with two imino, two amino or imino/amino chelating arms (dmimp, dmaiBrp, dmamp (Fig. 8), dpimp) afford complexes with the $Mn^{II}_2(\mu\text{-OPh})(\mu\text{-O}_2CR)_2^+$ core that have two vacant sites (one on each Mn) available for binding peroxide and Mn···Mn separation of 3.2–3.3 Å [68–70]. Based on ^{18}O isotopic labeling experiments, FAB-MS and electronic spectroscopy it has been proposed that these catalysts cycle between Mn_2^{III} and Mn_2^{IV} oxidation states to disproportionate H_2O_2 in DMF [68–71]. A similar behavior might explain the catalase activity exhibited by the (μ-phenoxo)(μ-carboxylato)dimanganese(II) complex formed with the N_2O_3 pentadentate phenol-based ligand bprol-^{t}Bu-p, $[Mn_2^{II}(\text{bprol-}^t\text{Bu-p})(\mu\text{-OAc})(H_2O)_2]^{2+}$ (Fig. 8), which possess two labile sites on each Mn ion [72]. This complex reacted without a lag period (the period of time prior to the beginning of the reaction) and at similar rate (Table 2, entry 14) as the other complexes with pentadentate phenol-based ligands having the N_4O donor set. Under the same reaction conditions, complexes of diaminophenolate ligands with two labile positions *trans* to each other and Mn···Mn separation of 3.598 Å, react at similar rate but after a lag period much longer than for the other phenolato-bridged complexes with intermetallic distance of 3.2–3.3 Å and two *cis* vacant sites [73]. It has been proposed that deformation of the initial core structure of the diaminophenolate complexes was required to provide two *cis* vacant sites to form active *cis*-$\{Mn^{III}(OH)\}_2$ and *cis*-$\{Mn^{IV}(=O)\}_2$ intermediates.

Phenolato-bridged diMn complexes of heptadentate ligands are much less efficient to disproportionate H_2O_2 than those of the pentadentate ones. The activity of $[Mn^{II}_2(bpmp)(O_2CR)_2]^+$, with R = Me or Ph, in acetonitrile is much lower than that of the $diMn^{II}$ complexes with the pentadentate diaminophenolate ligands [70,74]. However, $Mn^{II}_2(bpmp)Cl_2^+$, with a Mn···Mn distance of 3.923 Å exhibits much higher catalase activity, similar to that of the pentadentate diaminophenolate ligand [75]. EPR monitoring of the reaction in acetonitrile, showed that this complex employs $Mn^{II}Mn^{III}$ and $Mn^{III}Mn^{IV}$ oxidation states to catalyze H_2O_2 disproportionation. These results are quite different from those reported for phenolato-bridged diMn complexes formed with pentadentate ligands where the formation of a Mn^{IV}=O species in DMF solution had been observed during H_2O_2 disproportionation

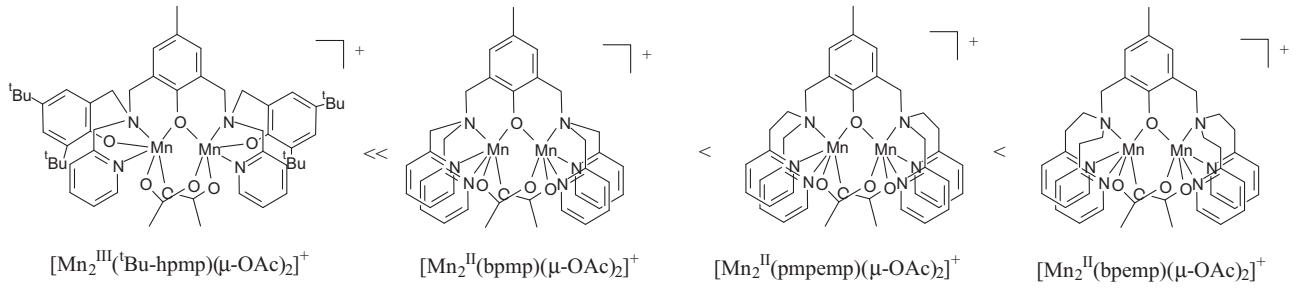

Fig. 6. Relative redox potentials of phenoxo-bridged Mn_2 complexes.

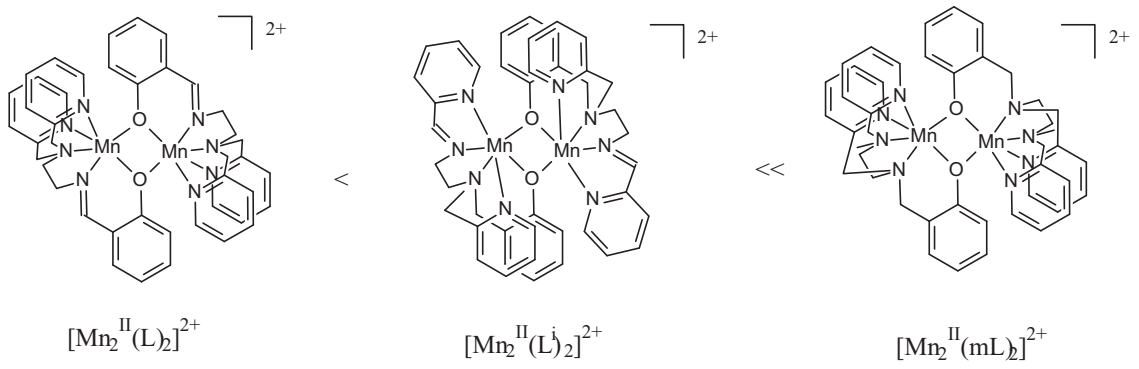

Fig. 7. Relative redox potentials of imino/phenolato and amino/phenolato Mn_2^{II} complexes. Adapted from Ref. [56].

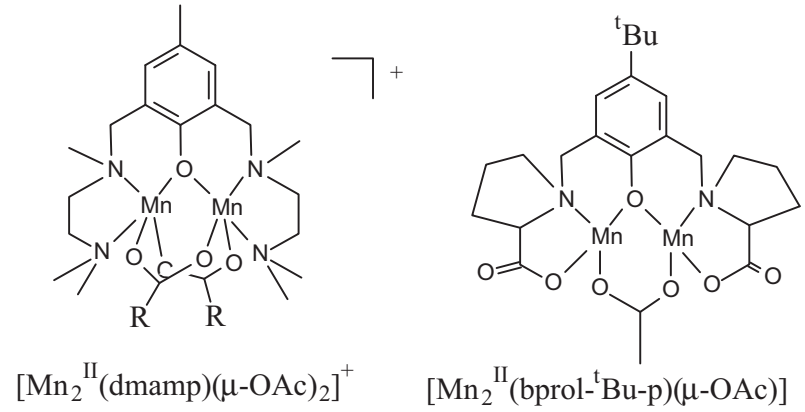

Fig. 8. Complexes with one and two vacant sites on each Mn ion that show similar CAT activity. The structure of $[Mn_2^{II}(bprol\text{-}^tBu\text{-}p)(\mu\text{-}OAc)]^{2+}$ is based on spectroscopic measurements.

[71]. The authors suggested that the long Mn···Mn distance in $Mn^{II}{}_2(bpmp)Cl_2{}^+$ may be flexible in solution, leading to facile formation of the peroxide adduct with $\mu_{1,2}$ bridging mode analogous to that proposed for asymmetric phenolato-bridged complexes that also cycle between $Mn^{II}Mn^{III}$ and $Mn^{III}Mn^{IV}$ levels (see below) [76]. The formation of such an adduct should be less favorable for the bis-acetato-bridged compound, that must proceed through shift of the acetato group.

5.3. Asymmetric MnCAT mimics

The two Mn ions of the active site of MnCAT possess the same NO_5 coordination environment. This symmetrical environment stabilizes the homovalent diMn core, which is consistent with the observed redox activity based on shuttling between Mn_2^{II}/Mn_2^{III} states during disproportionation of H_2O_2. Based on this fact, most MnCAT mimics have been designed using symmetrical ligands. However, diMn complexes of dissymmetric phenolato ligands disproportionate H_2O_2, although they involve $Mn_2^{II,III}/Mn_2^{III,IV}$ redox cycles in the catalysis. The finding that mixed valence dissymmetric phenolato-bridged diMn complexes can dismutate 100% of H_2O_2 [64,77], is in clear contrast to the previous affirmation [73] that hold that two electronically equivalent Mn ions were essential to dismutate H_2O_2 efficiently.

Hexadentate ligands have been used to obtain phenolato-bridged diMn complexes with a labile position on one of the Mn ions to facilitate the initial binding to the substrate. Such catalysts show turnover rates significantly higher than those of heptadentate ligands for which initial peroxide binding is enforced to occur through ligand exchange [77]. Bpbpmp provides an accessible coordination site on one Mn of the pair, occupied by one exogenous water or methanol molecule. Three complexes, $[Mn_2^{II}(bpbpmp)(\mu\text{-}O_2CR)_2(S)]^+$ (R = Me or Ph, S = water or methanol) and $[Mn_2^{II,III}(bpbpmp)(\mu\text{-}OAc)_2(H_2O)]^{2+}$ (Fig. 9) [78],

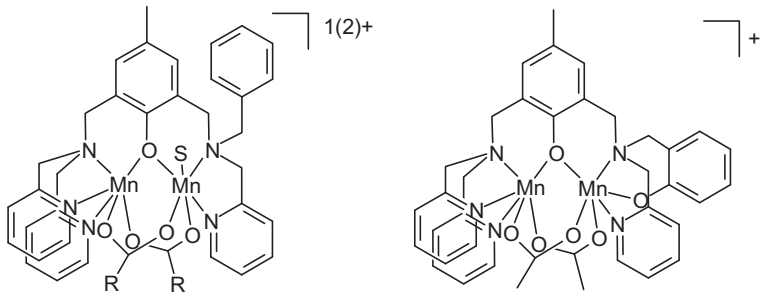

Fig. 9. Assymmetric phenoxo-bridged MnCAT mimics.

were obtained and characterized with water bound to Mn^{II} of the mixed valence complex. In these complexes the Mn···Mn distance is in the range of 3.42–3.44 Å in the reduced form, and 3.5 Å in the mixed valence complex, for which the shorter Mn—OPh bond length is compensated by the larger Mn—O—Mn angle. The asymmetry of the coordination of the Mn pair gives rise to an increased redox stability domain of the mixed valence state (Table 3, entries 9–10), larger than analogous $Mn_2^{II,III}$-tetrapyridinephenolato complexes, which are stable in a range of 0.51–0.54 V [79]. Bphpmp also affords a diMn complex with large stability domain of the $Mn_2^{II,III}$ state. This heptadentate N_5O_2 ligand has one soft side with a $N_{py}N_{py}N_{amine}$ donor set and one harder side $N_{py}N_{amine}O_{phenolate}$ to stabilize the dinuclear mixed-valence complex $[Mn_2^{II,III}(bphpmp)(\mu\text{-}OAc)_2]^+$ with Mn···Mn distance of 3.497 Å, stable over a range of about 1 V (Table 3, entry 7) [64].

Kinetic studies performed on the H_2O_2 disproportionation catalyzed by $[Mn_2^{II}(RCO_2)_2bpbpmp]^+$ (R = CH_3 or ph) and $[Mn_2^{II,III}(OAc)_2bpbpmp]^{2+}$ showed that the reaction is first order on both H_2O_2 and catalyst (Table 2, entry 15), with $[Mn_2^{II,III}(OAc)_2bpbpmp]^{2+}$ being more reactive than the Mn_2^{II} analogous [77]. The CAT-like reaction shuttles between $[Mn_2^{II,III}(O)bpbpmp(OAc)]^+$ and $[Mn_2^{III,IV}(O)_2(OAc)bpbpmp]^+$, the last formed upon initial oxidation of $[Mn_2^{II}(OAc)_2bpbpmp]^+$ [76]. In this reaction, the oxidized form of the catalyst dominates most of the reaction and therefore the slow redox step is the oxidation of H_2O_2, just the reverse as observed in the catalase from *L. plantarum* [21]. ^{18}O labeling experiments showed that the two O atoms of the Mn_2O_2 core come from a single H_2O_2 molecule and this was taken as evidence for the occurrence of a $\mu_{1,2}$ bridging mode of peroxide. An analogous observation had been made earlier for the H_2O_2 disproportionation by Mn_2^{II}/Mn_2^{III} alcoholato complexes [38]. These results showed that the same chemistry is performed by $Mn^{II}Mn^{III}$ and Mn_2^{II} sites, and it has been suggested this may be a general feature of the Mn_2O_2 cores and therefore possibly valid for the enzyme. Bpbpmp appears flexible enough to accommodate the $Mn^{IV}(\mu\text{-}O)_2Mn^{III}$ core by allowing a phenolate shift which frees some coordination positions [76]. A similar behavior might explain the catalase activity exhibited by the mixed-valence complex formed with the septadentate asymmetric ligand bphpmp, $[Mn_2^{II,III}(OAc)_2bphpmp]^{2+}$ (Ref. [64], Table 2, entry 6), and probably also $[Mn_2(O)_2(bpg)_2]^+$ (see Section 6) formed with *N*,*N*-bis(2-pyridylmethyl)glycine [80]. Such a situation may not be easily achievable with more conjugated phenolato-based ligands involving imine donors [71], which react slower and through a different redox cycle.

When O_2 evolution rates were compared under the same experimental conditions, it was found that the $Mn_2^{II,III}$ catalyst of bpbpmp is around 10 times more active than comparable Mn_2^{II} phenolato-bridged complexes with phenol-based pentadentate ligands, which in turn are much more active than the complex with the septadentate bpmp (Fig. 10) [70,71,74,77]. In the last case, there is no labile position to react with the substrate, so initial peroxide binding must occur through ligand exchange, probably an acetato-shift, and hence the reaction occurs after a long lag period. The fact that $[Mn_2^{II(or\ II,III)}(bpbpmp)(\mu\text{-}O_2CR)_2]^{1(2)+}$ shuttle between $Mn^{II}(\mu\text{-}O)Mn^{III}$ and $Mn^{IV}(\mu\text{-}O)_2Mn^{III}$ to disproportionate H_2O_2, and $[Mn_2^{II}(\mu\text{-}O_2CR)_2(N_4\text{-}O\text{-phenolate})]^+$ cycle between $[Mn^{III}(OH)]_2$ and $[Mn^{IV}(=O)]_2$ states [71], led to the conclusion that to disproportionate H_2O_2 these systems use the Mn_2 pairs, the redox potentials of which are the best adapted whatever the initial oxidation states of the Mn ions.

5.4. Macrocyclic MnCAT mimics

Several phenol-based macrocycles afford complexes with the $Mn_2^{II}(\mu\text{-}OPh)_2(\mu\text{-}OAc)_2$ core and Mn···Mn distances from 2.98 Å [81] to 3.37 Å [82] modulated by the flexibility of the alkyl linkers between two diiminophenolate moieties.

It has been proposed that these phenol-based macrocycle diMn complexes disproportionate H_2O_2 in DMF and 0 °C, through a catalytic mechanism involving interconversion between $Mn^{II}Mn^{III}(OH)$ and $Mn^{III}Mn^{IV}(=O)$ states. The increase of the macrocycle size results in a decrease of catalytic rate and a longer induction period. The different activity was attributed to the high substitution lability of the acetato ligand acting as bidentate to one metal atom in aqueous DMF for the complex with the shorter alkyl linkers against inertness of the bridging acetato group for the complex with the longer ones, and to the fact that the ligand with the shorter linkers is best suited for accommodating Mn in higher oxidation states [81]. For bis(μ-phenoxo)(μ-carboxylato)diMn complexes, the CAT activity showed dependence on the basicity of the bridging carboxylato, thus suggesting the importance of protonation prior to dissociation of the bridging carboxylato [83]. In dinuclear Mn^{II} complexes of macrocyclic ligands with two pendant arms the sixth coordination position of the Mn ions is occupied by the donor atom in the pendant arm [84,85]. Efficiency of these complexes to disproportionate H_2O_2 has been interpreted as the result of the dissociation of the arm from the Mn ion, where rapid dissociation of the arm results to an empty site that speeds up the CAT activity (Fig. 11).

5.5. Diphenoxo bridged MnCAT mimics

CAT activity of a few diphenoxo bridged Mn complexes has been examined. $[Mn^{III}_2(etsalim)_4(Hetsalim)_2]^{2+}$, with the two Mn ions separated by 3.37 Å, disproportionates H_2O_2 with saturation kinetics (Table 2, entry 8) and turnover numbers up to 3000, but the mechanism or even the oxidation states involved in catalysis were not established [86]. The CAT activity of Mn_2^{II} complexes with tripodal amine ligands with an N_3O donor set

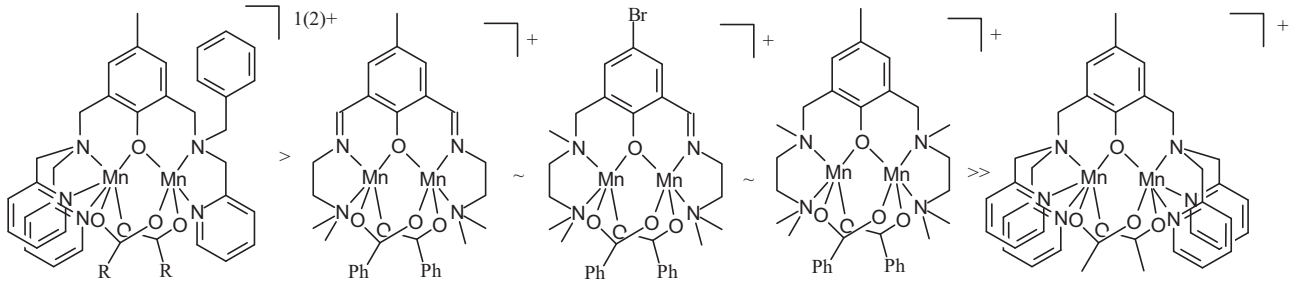

Fig. 10. Relative CAT activity of phenoxo-bridged diMn complexes.

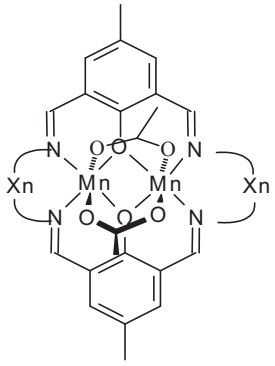

Fig. 11. Phenoxo-bridged diMn complexes of phenol-based macrocycles.

derived from bis(pyridylmethyl)(2-hydroxybenzyl)amine (bphba) has been reported [65]. The phenol moiety of the ligands leads to a bis(μ-phenoxo) bridging motif with Mn···Mn in the 3.39–3.49 Å range, leaving one vacant site at each Mn center occupied by chloride ions. These complexes show catalytic activity for H_2O_2 disproportionation (Table 2, entry 7) and introduction of electron-donating groups into the aromatic π-system leads to higher catalytic activity involving lower redox potentials.

6. Dimanganese complexes with oxo/carboxylato bridges

One of the most important structural features of MnCAT is the carboxylato bridge which is believed to be critical to H_2O_2 disproportionation. Among complexes with the same terminal ligands, the number of bridging acetato/oxo groups directly correlates with Mn oxidation states and CAT activity [54], i.e. two successive controlled potential oxidations of $[Mn_2^{II}(\mu\text{-OAc})_2(tpa)_2]^{2+}$ at 1.0 and 1.4 V (vs. SCE) allowed nearly quantitative formation of $[Mn_2^{III}(\mu\text{-O})(\mu\text{-OAc})(tpa)_2]^{3+}$ and $[Mn_2^{IV}(\mu\text{-O})_2(tpa)_2]^{4+}$, respectively, showing that each substitution of an acetato group by an oxo one is caused by an overall two-electron oxidation of the corresponding diMn complex [87]. Conversion of the $Mn_2^{II}(\mu\text{-OAc})_2{}^{2+}$ core into $Mn_2^{III}(\mu\text{-O})(\mu\text{-OAc})^{3+}$ implies a noticeable compression of bond lengths along the oxo-bridge, with Mn···Mn distance decreasing from 4.15 [88] to 3.25–3.29 Å [87,89–91]. This is illustrated by the shortening of the Mn···Mn distances from 4.13 Å in $[Mn^{II}(bpia)(\mu\text{-OAc})]_2{}^{2+}$, to 3.25 Å in $[Mn^{III}{}_2(bpia)_2(\mu\text{-}O)(\mu\text{-OAc})]^{3+}$ and 2.624 Å in $[Mn_2^{III,IV}(bpia)_2(\mu\text{-O})_2]^{2+}$ as the acetato groups are replaced by oxo groups and the Mn oxidation state increases [90]. $[Mn^{II}(bpia)(\mu\text{-OAc})]_2{}^{2+}$ disproportionates H_2O_2 (in DMF and 25 °C) with saturation kinetics (Table 2, entry 9), whereas $[Mn^{III}{}_2(bpia)_2(\mu\text{-}O)(\mu\text{-OAc})]^{3+}$, which converts into $[Mn_2^{III,IV}(bpia)_2(\mu\text{-O})_2]^{2+}$, showed second order kinetics and lower disproportionation rate, in CH_3CN and 25 °C, probably because the lower oxidation state of Mn favors dissociation of the acetato ligand for binding the substrate [87]. The same relation of acetato/oxo bridging ligands to Mn oxidation was found for triply bridged diMn complexes with tridentate ancillary N ligands. Owing to the presence of an additional acetato bridge with a more pronounced electron-donor character than pyridine, the oxidation potentials of bpea complexes are lower than those of the tpa complexes. $[Mn_2^{III}(\mu\text{-O})(\mu\text{-OAc})_2(bpea)_2]^{2+}$ and $[Mn_2^{IV}(\mu\text{-O})_2(\mu\text{-OAc})(bpea)_2]^{3+}$ have been efficiently generated by successive electrochemical oxidation of $[Mn_2^{II}(\mu\text{-OAc})_3(bpea)_2]^{+}$ at 0.9 and 1.2 V (vs. SCE), showing again that the two-electron oxidation of the diMn cores involves the substitution of an acetato group by an oxo one [92]. These triply bridged bpea complexes showed CAT activity, and $[Mn_2^{II}(\mu\text{-OAc})_3(bpea)_2]^{+}$ were far more active than $[Mn_2^{III}(\mu\text{-O})(\mu\text{-OAc})_2(bpea)_2]^{2+}$ and $[Mn_2^{III,IV}(\mu\text{-O})_2(\mu\text{-OAc})(bpea)_2]^{2+}$. For these complexes, spectroscopic evidence (EPR, UV–vis) pointed to an active system shuttling between $[Mn_2^{II}(\mu\text{-OAc})_2(bpea)_2(H_2O)_2]^{2+}$ and $[Mn_2^{III}(\mu\text{-OAc})_2(bpea)_2(OH)_2]^{2+}$ during catalysis, with the two-electron oxidation + acetato/oxo exchange competing with H_2O_2 disproportionation. It was suggested that the lower oxidation state of Mn ions and the lower charge of the core cation of $[Mn_2^{II}(\mu\text{-OAc})_3(bpea)_2]^{+}$ favor dissociation of acetato for binding the substrate and result in CAT activity higher than for the diMn species in higher oxidation states [93]. Complexes $[Mn_2^{III}(\mu\text{-}O_2CR)_2(\mu\text{-O})(bipy)_2(H_2O)_2]^{2+}$ and $[Mn_2^{III}(\mu\text{-}O_2CR)_2(\mu\text{-O})(phen)_2(H_2O)_2]^{2+}$ (R = $ClCH_2$ or CH_3), with Mn···Mn distance of 3.16 Å, also showed CAT activity in CH_3CN, favored by the presence of one labile water molecule coordinated to each Mn center [94]. Although kinetic parameters were not determined, H_2O_2 disproportionation turnovers of 160–280 were found after 1 h. Spectroscopic evidence indicated that these catalysts employ Mn_2^{II}/Mn_2^{III} oxidation states during catalysis and carboxylato bridges are preserved during the catalytic cycle. Since in these complexes the two water molecules are *trans* to each other, it was proposed that substitution of a water ligand by peroxide occurs in a first step, with peroxide bound to Mn as a terminal ligand stabilized by hydrogen bonding with the oxo or carboxylato ligand.

The carboxylato arms of tripodal amine ligands were used to mimic Glu35 and Glu148 of CAT from *L. plantarum* when bound to Mn or Glu178 when unbound (Fig. 1), which have been postulated to act as proton acceptor groups during H_2O_2 disproportionation [95]. The influence of the carboxylato content of three tripodal amine ligands (Hbpg, H_2pda and H_3nta) on the properties and CAT activity of complexes with bis(μ-oxo)bis-manganese(III,III) and (III,IV) cores has been evaluated [96]. It was found that replacement of pyridine by carboxylato has a dramatic influence on the redox potentials of the Mn_2O_2 core (Table 1, entries 8–10). The effect of pyridine/CO_2^- substitution of an in-plane pyridine (about 300 mV) was more prominent than replacement of a second axial pyridine (about 60 mV) by a carboxylato, probably due to the more distant binding of CO_2^- to Mn on the elongation Jean–Teller axis. ESI-MS studies of the reaction of these complexes with ^{18}O-labeled H_2O_2 showed that they incorporate oxo-ligands from H_2O_2. CAT activity of these complexes is favored by the lower oxidation state of

Mn ($Mn_2^{III} > Mn_2^{III,IV}$) and by the increasing content of carboxylato ligands. Therefore, each pyridine/CO_2^- substitution enhanced the H_2O_2 disproportionation rate fivefold, and this increase was not originated by the shift in redox potentials that were markedly reduced on the first pyridine/CO_2^- substitution but far less on the second one (Table 1, entries 8–10 and Table 2, entries 16–18). It had been postulated that, owing to their intrinsic lability, the carboxylato ligands dissociate, opening a coordination site for an incoming substrate molecule [92,97]. However, the fact that the rate enhancement produced by addition of Et_3N had a lesser effect as the number of carboxylato ligands increased has suggested that the carboxylato ligands play the role of internal bases assisting H_2O_2 dismutation [80,96]. This conclusion is consistent with the facts that in DMF (a stronger proton acceptor than acetonitrile) $[Mn_2^{III,IV}(\mu\text{-}O)_2(tpa)_2]^{3+}$, $[Mn_2^{III,IV}(\mu\text{-}O)_2(cyclam)_2]^{3+}$ and $[Mn_2^{III,IV}(\mu\text{-}O)_2(bpg)_2]^{+}$ disproportionate H_2O_2 with similar rate and addition of pyridinium bromide as a proton donor decreased the rate of O_2 evolution while the spectral properties of the diMn compounds remained unchanged [80]. These results also agree with the fact that $[Mn_2^{III,IV}(\mu\text{-}O)_2(\mu\text{-}OAc)(Me_3\text{-}tacn)(bipy)]^{2+}$ reacts twice as fast as $[Mn_2^{III,IV}(\mu\text{-}O)_2(\mu\text{-}OAc)(Me_3\text{-}tacn)(OAc)_2]^{2+}$ in aqueous acetate buffer of pH 4.6 (Table 2, entries 10–11), showing that protonation of terminal carboxylato results in lower CAT activity [98].

The influence of the carboxylato coordination mode of bpmapa and pbpmapa ligands on the catalase activity of $diMn^{II}$ complexes with the same coordination sphere $N_3O_{4(3)}$ and Mn···Mn distance of 3.69 Å, has been studied [99]. These complexes differ in the coordination mode of carboxylato groups: $\mu_{1,1}$ bidentate vs. monodentate bridging, as shown in Fig. 12, and show ability to catalyze H_2O_2 disproportionation involving $Mn_2^{III,IV}$ species.

Compound with the $\mu_{1,1}$ bidentate carboxylato bridge exhibited higher activity (r_0 = 1.26 mL O_2 min^{-1}) than those with monodentate bridging carboxylato ligands (r_0 = 0.185–0.076 mL O_2 min^{-1}). Based on spectroscopic studies, relative activities and nitrogenous base influences on activity, the authors concluded that in these complexes the carboxylato bridge acts as an internal base in H_2O_2 disproportionation, and that the basicity of the carboxylato increases as the O—C—O angle and the distance between the weakly bound oxygen of the bridging carboxylato to the Mn ion decrease. Thus, a $\mu_{1,1}$ bidentate carboxylato bridge that has small O—C—O angle and short Mn—O distance exhibits stronger basicity and leads to a more active CAT mimic than a monodentate bridging one.

Another group of complexes with the bis(μ-oxo)$Mn_2^{III,IV}$ core obtained with X-bispicMe$_2$en disproportionate H_2O_2 in aqueous medium [100]. These tetradentate N_4-ligands afford $[Mn_2^{III,IV}(\mu\text{-}O)_2(X\text{-}bispicMe_2en)_2]^{3+}$, that in phosphate buffer, disproportionates H_2O_2 with second order kinetics (Table 2, entry 19). From EPR and UV–vis studies it was proposed that the CAT activity

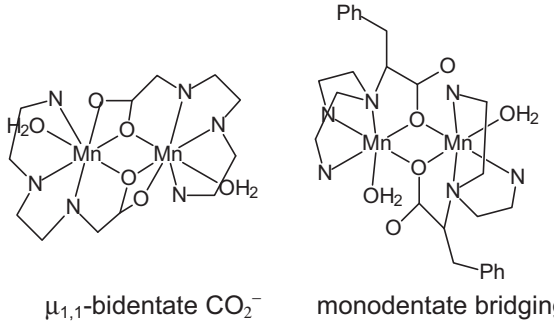

Fig. 12. Carboxylato coordination mode in diMn complexes of bpmapa and pbpmapa.

occurs via the Mn_2^{III}/Mn_2^{IV} states, with formation of the active catalyst during the lag period either by dismutation or one-electron reduction of the starting complex. The observed rise in CAT activity with increasing electron-withdrawing character of the substituent (Table 2, entry 19) [100] was proposed to be the result of increasing potentials of the $Mn_2^{III}/Mn_2^{III,IV}$ and $Mn_2^{III,IV}/Mn_2^{IV}$ couples by about 0.2–0.35 V on going from Me to NO_2 (Table 1, entry 11) [100,101]. This fact is consistent with oxidation of H_2O_2 occurring in the slow redox step of the catalytic cycle.

Recently, a dichloride-bridged diMn complex, $[Mn^{II}_2(\mu\text{-}Cl)_2tpa_2]^{2+}$, was synthesized as a functional complex of the chloride inhibited MnCAT [102,103]. ESI-MS, UV–vis and EPR spectroscopies showed that upon reaction with excess H_2O_2 the complex transforms into $[Mn^{III}Mn^{IV}(\mu\text{-}O)_2tpa_2]^{3+}$ and disproportionates H_2O_2 through a catalytic cycle involving $Mn^{III}Mn^{IV}$ and $Mn^{II}Mn^{III}$ oxidation states, with k_{cat} 107 s^{-1} and K_M 3.1 M in CH_3CN [102]. It was observed that H_2O molecules compete with H_2O_2 for the active site of the catalyst resulting in a significant inhibitory effect, with K_M and k_{cat} decreased twice and 50 times, respectively, in the presence of water. Similarly, $[Mn^{II}_2(\mu\text{-}Cl)(\mu\text{-}OAc)bpeaph_2]^{2+}$ converts into $[Mn^{III}Mn^{IV}(\mu\text{-}O)_2bpeaph_2]^{3+}$ upon addition of H_2O_2 and disproportionates H_2O_2 employing $Mn^{III}Mn^{IV}$ and $Mn^{II}Mn^{III}$ levels, with k_{cat} 1.74 s^{-1} in aqueous CH_3CN [104]. The high CAT activity observed for $[Mn^{III}Mn^{IV}(\mu\text{-}O)_2tpa_2]^{3+}$ in anhydrous medium agrees with that of $[Mn^{IV}(\mu\text{-}O)(salpn)]_2$, a compound that cycles between the Mn_2^{III} and Mn_2^{IV} oxidation levels, with k_{cat} 250 s^{-1} and K_M 250 mM [105,106]. For this complex, the CAT reaction proceeds with exchange of the bridging oxo groups and both the resultant μ-oxo atoms originate from the same peroxide molecule. Although $[Mn^{IV}(\mu\text{-}O)(salpn)]_2$ and $[Mn^{III}Mn^{IV}(\mu\text{-}O)_2tpa_2]^{3+}$ are among the more reactive catalysts for H_2O_2 disproportionation, the high K_M values reflect their poor affinity for the substrate.

7. Mononuclear Mn catalysts

A number of mononuclear Mn complexes have shown CAT activity. The efficiency of these systems seems to be related to the presence of at least one labile coordination position on the Mn ion [107]. $[Mn^{II}(bimindH)Cl_2]$ showed CAT activity with second order k of 4.12 M^{-1} s^{-1} in EtCN [108]. A related complex, $[Mn^{II}(Hind)Cl_2]$ disproportionates H_2O_2 with second order kinetics and k of 1.55 M^{-1} s^{-1} in CH_3CN, in the presence of nitrogenous bases. Interestingly, in aqueous solution of pH 9.6 at 21 °C the complex showed saturation kinetics with k_{cat} = 38 s^{-1} and K_M = 489 mM [109]. The lack of observation of lag period in the aqueous basic medium points to a rapid formation of the dimer required for the CAT activity, or better, that the dimer is already present in solution when H_2O_2 is added. Mn complex of salbutOH showed catalase activity in methanol and DMF, with k_{cat} = 1.6 M^{-2} s^{-1} and 5.6 M^{-1} s^{-1}, respectively [110]. This complex acts as scavenger of H_2O_2 and O_2^-, and this valuable conjunction of properties was proposed to result from the conversion of $[Mn^{IV}(salbutO)X]$ into $[Mn^{III}(salbutO)]_2$ in equilibrium with its monomer $[Mn^{III}(salbutO)]$ [110]. HPClNOL yields mononuclear $[Mn^{II}(PClNOL)(\eta_1\text{-}NO_3)(\eta_2\text{-}NO_3)]$ [111]. The complex is soluble in water with the dimeric $[Mn_2^{II}(NO_3)_3(PClNOL)_2]^+$ form being predominant in buffered solution of pH 7. The complex disproportionates H_2O_2 with the highest CAT activity observed at pH 7.2 and protons induced inactivation at pH 4.6 [112]. Based on EPR, UV–vis and ESI-MS the CAT cycle was proposed to involve $[Mn_2^{III,IV}(\mu\text{-}O)_2(PClNOL)_2]^+$ and $[Mn_2^{II,III}(\mu\text{-}O)(PClNOL)_2]^+$, the last being unstable in protic medium to yield final mononuclear Mn^{II} species. The $Mn_2^{III,IV}$ species is the major one during the catalytic cycle, so its reduction should be the slow step. $[Mn^{II}(chedam)(bipy)(H_2O)]$ offers one labile site for binding the substrate and shows CAT activity in the presence of imidazol

e (in the absence of the base the complex is inactive) with a moderate rate of oxygen evolution of 0.017 mmol O_2 s^{-1} [113]. Complexes $Mn^{II}(X\text{-ind})_2$ constitute an exceptional case exhibiting CAT activity even when the six coordination sites of Mn^{II} are occupied by two tridentate ligands [114]. Disproportionation of H_2O_2 by these complexes showed saturation kinetics on $[H_2O_2]_0$ with values of k_{cat} of 0.06–0.26 s^{-1} and K_M of 19–82 mM, for ind and 4Me-ind, respectively, in DMF and 20 °C.

Mn-salen complexes have dual SOD/CAT activity, an advantageous property since SOD activity alone would produce cytotoxic H_2O_2 [115,116]. However, most salen complexes lose activity in a few minutes under the conditions of the catalase assay [117]. A Mn-salen complex bearing an ureido group as an auxiliary placed over the Mn-salen plane exhibited enhanced CAT-like activity compared to the original Mn-salen complexes in neutral aqueous medium [118], with initial rate of 0.5 mM min^{-1} (k_{cat} = 8.3 s^{-1}) and 32 turnovers. In order to improve the water solubility of the catalyst, Mn^{III}-salen type complexes were conjugated with cyclodextrines [119]. The conjugation to the dextrine gives these complexes a marked enhancement of water solubility compared to Mn-salen compounds and show CAT activity about twice that of simple complexes, with k_{cat} 0.2–0.4 s^{-1} and K_M of 5–6 mM. Water soluble anionic $[Mn(SO_3\text{-salpn(OH)})]^-$ disproportionated up to 250 equivalents of H_2O_2 and showed improved CAT activity with initial turnover rates of 3 s^{-1} at pH 8 [120].

8. Toward biological applications

In a variety of pathological situations the production of peroxide overwhelms the activity of endogenous defense systems and results in cell damage. H_2O_2 has been postulated as playing a role in acute respiratory distress syndrome, ischemia-reperfusion injury, atherosclerosis, neurodegenerative diseases and cancer [4]. As CAT mimics act as H_2O_2-scavengers, their application to attenuate hydrogen peroxide-induced injury has been proposed in cases where oxidative stress is important in the mechanism of a disease. However, the use of CAT mimics as therapeutic agents has shown limitations because of their short half-life in the circulation, antigenicity, high costs, and large size that disables the enzyme to cross the cell membranes. To overcome these limitations, low molecular weight Mn-based catalytic antioxidants have been tested in several oxidative stress models in vivo [121–125]. All tested catalysts are mononuclear complexes, primarily designed as SOD scavengers. Among them, Mn-porphyrins and Mn-salen compounds have been the most extensively studied. These complexes are non-selective antioxidants, which catalyze H_2O_2 and O_2^- disproportionation, and are also active toward $ONOO^-$ and lipid peroxides [121]. Although protecting cells from H_2O_2-mediated toxicity, the CAT activity of these compounds is low (less than 1% of native CAT) [126]. The slow rates at which these catalysts scavenge H_2O_2 can result from their low stability under conditions of the CAT assays (especially in the case of Mn-salen compounds, as mentioned in the previous section) and the lack of structural analogies with the active site of MnCAT. These catalytic antioxidants have been proposed to react through a mechanism involving mononuclear Mn^V=O species [118,127] or through formation of dimeric species in solution [128], which are certainly different from that of the native enzyme. Therefore, testing the CAT activity of diMn complexes in biological systems is still a vacant research area. In the search of diMn mimics with higher stability and antioxidant activity in aqueous medium, it has been recently reported that 3-Me-5-SO_3-salpentOH affords a water soluble diMn complex with a triply bridged bis(μ-alkoxo)($\mu_{1,3}$-carboxylato)$diMn^{III}$ core that is highly efficient to disproportionate H_2O_2 in aqueous solution of pH ≥ 8.5 [129]. This compound, catalyzes dismutation of H_2O_2 with saturation kinetics on substrate and k_{cat}/K_M = 1600 s^{-1} M^{-1}, the high efficiency of which is the consequence of its high affinity for peroxide (K_M = 6.6 mM). Since efficient CAT activity and substrate affinity are only achieved at high pH, it has been proposed that the external base contributes to retain the integrity of the bis(μ-alkoxo) doubly bridged diMn core and favors the formation of the catalyst-peroxide adduct. The same dependence of k_{cat} and K_M on pH was observed for Y42F LPC, a mutant of *L. plantarum* catalase, where replacement of Tyr42 by phenylalanine disrupts the hydrogen-bonded web and leaves the double solvent bridged diMn core unprotected [20]. Water soluble diMn mimics of higher stability and improved activity at physiological pH have not been reported up to date.

9. Concluding remarks

Based on the structure, kinetic parameters and redox potentials of MnCAT mimics, several general features have merged, the more relevant being the following: (i) Catalytic rates of H_2O_2 disproportionation by diMn complexes depend not only on redox potentials, as shown by the similar k_{cat} values observed for complexes with large difference in redox potentials, but are strongly affected by the presence of an intramolecular base to assist in deprotonation of H_2O_2. (ii) The affinity for the substrate is enhanced for catalysts with vacant sites on the Mn ion, just as shown by the trend in K_M values and lag periods. (iii) The fact that redox potentials of a number of mimics are in the same range but employ different redox cycles to dismutate H_2O_2, indicates that the oxidation states of Mn during the catalytic cycle also depend on structural factors (i.e. Mn···Mn distance, chelate ring size, ligand flexibility, vacant sites) that, in turn, are key for controlling the peroxide binding mode. (iv) In aqueous medium, protonation of the ligands bridging the two Mn ions causes the catalyst inactivation. Therefore, it is essential to control the reaction pH to preserve the integrity of the diMn core, and hence, the catalytic activity.

Acknowledgments

S.S. is grateful for the financial support from the National University of Rosario, CONICET and the National Agency for Sciences Promotion. C.H. thanks J.P. Tuchages for giving her the opportunity to build a collaboration with Prof. S. Signorella.

References

[1] B. Halliwell, J.M.C. Gutteridge, Methods Enzymol. 186 (1990) 1.
[2] B. Halliwell, J.M.C. Gutteridge, Free Radicals in Biology and Medicine, Oxford Univ Press, 1999.
[3] S.J. Stohs, D. Bagchi, Free Radic. Biol. Med. 18 (1995) 321.
[4] L.M. Sayre, G. Perry, M.A. Smith, Chem. Res. Toxicol. 21 (2008) 172.
[5] V. Costa, P. Moradas-Ferreira, Mol. Aspects Med. 22 (2001) 217.
[6] M. Valko, D. Leibfritz, J. Moncol, M.T. Cronin, M. Mazur, J. Telser, Int. J. Biochem. Cell Biol. 39 (2007) 44.
[7] D.S. Warner, H. Sheng, I. Batinić-Haberle, J. Exp. Biol. 207 (2004) 3221.
[8] J. Bravo, M.J. Mate, T. Schneider, J. Switala, K. Wilson, P.C. Loewen, I. Fita, Proteins 34 (1999).
[9] S.V. Antonyuk, W.R. Melik-Adamiyan, V.R. Popov, V.S. Lamzin, P.D. Hempstead, P.M. Harrison, P.J. Artymiuk, V.V. Barynin, Crystallogr. Rep. 45 (2000) 105.
[10] V.V. Barynin, M.M. Whittaker, S.V. Antonyuk, V.S. Lamzin, P.M. Harrison, P.J. Artymiuk, J.W. Whittaker, Structure 9 (2001) 725.
[11] G.C. Dismukes, Chem. Rev. 96 (1996) 2909.
[12] A.J. Wu, J.E. Penner-Hahn, V.L. Pecoraro, Chem. Rev. 104 (2004) 903.
[13] G.S. Algood, J.I. Perry, J. Bacteriol. 168 (1986) 563.
[14] V.V. Barynin, A.J. Grebenko, Dokl. Akad. Nauk. SSSR 286 (1986) 461.
[15] Y. Kono, J. Fridovich, J. Biol. Chem. 258 (1983) 6015.
[16] J. Mizobata, M. Kagawa, N. Murakoshi, E. Kusaka, K. Kameo, Y. Kawata, J. Nagai, Eur. J. Biochem. 267 (2000) 4264.
[17] V.V. Barynin, P.D. Hempstead, A.A. Vagin, S.V. Antonyuk, W.R. Melik-Adamiyan, V.S. Lamzin, P.M. Harrison, P.J. Artymiuk, J. Inorg. Biochem. 67 (1997) 196.
[18] S.V. Khangulov, P.J. Pessiki, V.V. Barynin, D. Ash, G.C. Dismukes, Biochemistry 34 (1995) 2015.

[19] T.L.T.M.S. Stemmler Jr., J.I. Goldstein, D.E. Ash, T.E.D.M.K. Elgren Jr., J.E. Penner-Hahn, Biochemistry 36 (1997) 9847.
[20] M.M. Whittaker, V.V. Barynin, T. Igarashi, J.W. Whittaker, Eur. J. Biochem. 270 (2003) 1102.
[21] M. Shank, V. Barynin, G. Dismukes, Biochemistry 33 (1994) 15433.
[22] J.E. Penner-Hahn, in: V.L. Pecoraro (Ed.), Manganese Redox Enzymes, VCH, New York, 1992.
[23] J.E. Penner-Hahn, V.L. Pecoraro, in: V.L. Pecoraro (Ed.), Manganese Redox Enzymes, VCH, New York, 1992.
[24] S.V. Khangulov, V.V. Barynin, S.V. Antonyuk-Barynina, Biochim. Biophys. Acta Bioinerg. 1020 (1990) 25.
[25] G.S. Waldo, J.E. Penner-Hahn, Biochemistry 34 (1995) 1507.
[26] M.M. Whittaker, V.V. Barynin, S.V. Antonyuk, J.W. Whittaker, Biochemistry 38 (1999) 9126.
[27] T. Amo, H. Atomi, T. Imanaka, J. Bacteriol. 184 (2002) 3305.
[28] G.S. Allgood, J.J. Perry, J. Bacteriol. 168 (1986) 563.
[29] M. Kagawa, N. Murakoshi, Y. Nishikawa, N. Matsumoto, Y. Kurata, J. Mizobata, Y. Kawata, J. Nagai, Arch. Biochem. Biophys. 362 (1999) 346.
[30] H. Biava, C. Palopoli, C. Duhayon, J.-P. Tuchagues, S. Signorella, Inorg. Chem. 48 (2009) 3205.
[31] A.E.M. Boelrijk, G.C. Dismukes, Inorg. Chem. 39 (2000) 3020.
[32] A.E.M. Boelrijk, S.V. Khangulov, G.C. Dismukes, Inorg. Chem. 39 (2000) 3009.
[33] A. Gelasco, M.L. Kirk, J.W. Kampf, V.L. Pecoraro, Inorg. Chem. 36 (1997) 1829.
[34] A. Gelasco, V.L. Pecoraro, J. Am. Chem. Soc. 115 (1993) 7928.
[35] P.J. Pessiki, G.C. Dismukes, J. Am. Chem. Soc. 116 (1994) 898.
[36] P.J. Pessiki, S.V. Khangulov, D.M. Ho, G.C. Dismukes, J. Am. Chem. Soc. 116 (1994) 891.
[37] S. Signorella, J.-P. Tuchagues, D. Moreno, C. Palopoli, in: J.G. Hughes, A.J. Robinson (Eds.), Inorganic Biochemistry Research Progress, Nova Sci. Publ. Inc., New York, 2008.
[38] A. Velasco, S. Bensiek, V.L. Pecoraro, Inorg. Chem. 37 (1998) 3301.
[39] L.A. Berben, J.C. Peters, Inorg. Chem. 47 (2008) 11669.
[40] M.G.B. Drew, C.J. Harding, V. McKee, G.G. Morgan, J. Nelson, J. Soc. Chem., Chem. Commun. (1995) 1035.
[41] S. Durot, C. Policar, F. Cisnetti, F. Lambert, J.-P. Renault, G. Pelosi, G. Blain, H. Korri-Youssoufi, J.-P. Mahy, Eur. J. Inorg. Chem. (2005) 3513.
[42] D. Moreno, C. Palopoli, V. Daier, S. Shova, L. Vendier, M. González-Sierra, J.-P. Tuchagues, S. Signorella, Dalton Trans. (2006) 5156.
[43] S. Signorella, A. Rompel, K. Buldt-Karentzopoulos, B. Krebs, V.L. Pecoraro, J.-P. Tuchagues, Inorg. Chem. 46 (2007) 10864.
[44] H. Biava, C. Palopoli, S. Shova, M.D. Gaudio, V. Daier, M. González-Sierra, J.-P. Tuchagues, S. Signorella, J. Inorg. Biochem. 100 (2006) 1660.
[45] C. Palopoli, B. Chansou, J.-P. Tuchagues, S. Signorella, Inorg. Chem. 39 (2000) 1458.
[46] C. Palopoli, M. González-Sierra, G. Robles, F. Dahan, J.-P. Tuchagues, S. Signorella, J. Chem. Soc., Dalton Trans. (2002) 3813.
[47] V. Daier, H. Biava, C. Palopoli, S. Shova, J.-P. Tuchagues, S. Signorella, J. Inorg. Biochem. 98 (2004) 1806.
[48] J.J. Zhang, Q.H. Luo, C.Y. Duan, Z.L. Wang, Y.H. Mei, J. Inorg. Biochem. (2001) 573.
[49] S. Blanchard, G. Blondin, E. Rivière, M. Nierlich, J.-J. Girerd, Inorg. Chem. 42 (2003) 4568.
[50] P. Huang, A. Magnuson, R. Lomoth, M. Abrahamsson, M. Tamm, L. Sun, B.v. Rotterdam, J. Park, L. Hammarström, B. Åkermark, S. Styring, J. Inorg. Biochem. 91 (2002) 159.
[51] M.F. Anderlund, J. Högblom, W. Shi, P. Huang, L. Eriksson, H. Weihe, S. Styring, B. Åkermark, R. Lomoth, A. Magnuson, Eur. J. Inorg. Chem. (2006) 5033.
[52] R. Lomoth, P. Huang, J. Zheng, L. Sun, L. Hammarström, B. Akermark, S. Styring, Eur. J. Inorg. Chem. (2002) 2965.
[53] P. Kurz, M.F. Anderlund, N. Shaikh, S. Styring, P. Huang, Eur. J. Inorg. Chem. (2008) 762.
[54] M.N. Collomb, A. Deronzier, Eur. J. Inorg. Chem. (2009) 2025.
[55] Y. Gultneh, B. Ahvazi, A.R. Kahn, R.J. Butcher, J.-P. Tuchagues, Inorg. Chem. 34 (1995) 3633.
[56] L. Sabater, C. Hureau, G. Blain, R. Guillot, P. Thuéry, E. Rivière, A. Aukauloo, Eur. J. Inorg. Chem. (2006) 4324.
[57] C. Hureau, E. Anxolabéhère-Mallart, M. Nierlich, F. Gonnet, E. Rivière, G. Blondin, Eur. J. Inorg. Chem. (2002) 2710.
[58] C. Hureau, L. Sabater, E. Anxolabéhère-Mallart, M. Nierlich, M.-F. Charlot, F. Gonnet, E. Rivière, G. Blondin, Chem. Eur. J. 10 (2004) 1998.
[59] Y. Gultneh, A. Farooq, S. Liu, K.D. Karlin, J. Zubieta, Inorg. Chem. 31 (1992) 3607.
[60] Y. Gultneh, Y.T. Tesema, T.B. Yisgedu, R.J. Butcher, G. Wang, G.T. Yee, Inorg. Chem. 45 (2006) 3023.
[61] T.K. Lal, R. Mukherjee, Inorg. Chem. 37 (1998) 2373.
[62] H. Torayama, T. Nishide, H. Asada, M. Fujiwara, T. Matsushita, Polyhedron 17 (1998) 105.
[63] Y. Gultneh, Y.T. Tesema, B. Ahvazi, T.B. Yisgedu, R.J. Butcher, J.-P. Tuchagues, Inorg. Chim. Acta 359 (2006) 4463.
[64] P. Karsten, A. Neves, A.J. Bertoluzzi, J. Strähle, C. Maichle-Mössmer, Inorg. Chem. Commun. 5 (2002) 434.
[65] N. Reddig, D. Pursche, M. Kloskowski, C. Slinn, S.M. Baldeau, A. Rompel, Eur. J. Inorg. Chem. (2004) 879.
[66] A. Magnuson, P. Liebisch, J. Högblom, M.F. Anderlund, R. Lomoth, W. Meyer-Klaucke, M. Haumann, H. Dau, J. Inorg. Biochem. 100 (2006) 1234.
[67] G. Eilers, C. Zettersten, L. Nyholm, L. Hammarström, R. Lomoth, Dalton Trans. (2005) 1033.
[68] H. Sakiyama, H. Tamaki, M. Kodera, N. Matsumoto, H. Okawa, J. Chem. Soc., Dalton Trans. (1993) 591.
[69] C. Higuchi, H. Sakiyama, H. Okawa, R. Isobe, D.E. Fenton, J. Chem. Soc., Dalton Trans. (1994) 1097.
[70] C. Higuchi, H. Sakiyama, H. Okawa, D.E. Fenton, J. Chem. Soc. Dalton Trans. (1995) 4015.
[71] H. Sakiyama, H. Okawa, R. Isobe, J. Chem. Soc., Chem. Commun. (1993) 882.
[72] J. Kaizer, R. Csonka, G. Speier, React. Kinet. Catal. Lett. 94 (2008) 157.
[73] H. Okawa, H. Sakiyama, Pure Appl. Chem. 67 (1995) 273.
[74] H. Sakiyama, H. Ōkawa, M. Suzuki, J. Chem. Soc. Dalton (1993) 3823.
[75] Y. Sasaki, T. Akamatsu, K. Tsuchiya, S. Ohba, M. Sakamoto, Y. Nishida, Polyhedron 17 (1998) 235.
[76] L. Dubois, R. Caspar, L. Jacquamet, P.-E. Petit, M.-F. Charlot, C. Baffert, M.-N. Collomb, A. Deronzier, J.-M. Latour, Inorg. Chem. (2003) 4817.
[77] L. Dubois, D.-F. Xiang, X.-S. Tan, J.-M. Latour, Eur. J. Inorg. Chem. (2005) 1565.
[78] L. Dubois, D.-F. Xiang, X.-S. Tan, J. Pécaut, P. Jones, S. Baudron, L.L. Pape, J.-M. Latour, C. Baffert, S. Chardon-Noblat, M.-N. Collomb, A. Deronzier, Inorg. Chem. 42 (2003) 750.
[79] M. Suzuki, M. Mikuriya, S. Murata, A. Uehara, H. Oshio, S. Kida, K. Saito, Bull. Chem. Soc. Jpn. 60 (1987) 4305.
[80] Y. Nishida, T. Akamatsu, K.K. Tsuchia, M. Sakamoto, Polyhedron 13 (1994) 2251.
[81] T. Aono, H. Wada, M. Yonemura, M. Ohba, H. Ōkawa, D.E. Fenton, Dalton Trans. (1997) 1527.
[82] H. Wada, K. Motoda, M. Ohba, H. Sakiyama, N. Matsumoto, H. Okawa, Bull. Chem. Soc. Jpn. 68 (1995) 1105.
[83] T. Nagata, J. Mizukami, J. Chem. Soc. Dalton Trans. (1995) 2825.
[84] M. Qian, S. Gou, S. Chantrapromma, S.S.S. Raj, H.K. Fun, Q. Zeng, Z. Yu, X. You, Inorg. Chim. Acta 305 (2000) 83.
[85] M. Qian, S. Gou, Z. Yu, H. Ju, Y. Xu, C. Duan, X. You, Inorg. Chim. Acta 317 (2001) 157.
[86] M.D. Godbole, M. Kloskowski, R. Hage, A. Rompel, A.M. Mills, A.L. Spek, E. Bouwman, Eur. J. Inorg. Chem. (2005) 304.
[87] M.-N. Collomb, C. Mantel, S. Romain, C. Duboc, J.-C. Leprêtre, J. Pécaut, A. Deronzier, Eur. J. Inorg. Chem. (2007) 3179.
[88] H. Oshio, E. Ino, I. Mogi, T. Ito, Inorg. Chem. 32 (1993) 5697.
[89] N. Arulsamy, J. Glerup, A. Hazell, D.J. Hodgson, C.J. McKenzie, H. Toftlund, Inorg. Chem. 33 (1994) 3023.
[90] M.U. Triller, W.Y. Hsieh, V.L. Pecoraro, A. Rompel, B. Krebs, Inorg. Chem. 41 (2002) 5544.
[91] K.J. Oberhausen, R.J. O'Brien, J.F. Richardson, R.M. Buchanan, R. Costa, J.M. Latour, H.L. Tsai, D.N. Hendrickson, Inorg. Chem. 32 (1993) 4561.
[92] R. Tagore, H. Chen, R.H. Crabtree, G.W. Brudvig, J. Am. Chem. Soc. 128 (2006) 9457.
[93] I. Romero, L. Dubois, M.N. Collomb, A. Deronzier, J.M. Latour, J. Pecaut, Inorg. Chem. 41 (2002) 1795.
[94] G. Fernández, M. Corbella, M. Alfonso, H. Stoeckl-Evans, I. Castro, Inorg. Chem. 43 (2004) 6684.
[95] J.W. de Boer, W.R. Browne, B.L. Feringa, R. Hage, C.R. Acad. Sci. Ser. II C: Chim. 10 (2007) 341.
[96] L. Dubois, J. Pécaut, M.-F. Charlot, C. Baffert, M.-N. Collomb, A. Deronzier, J.-M. Latour, Chem. Eur. J. 14 (2008) 3013.
[97] R. Tagore, R.H. Crabtree, G.W. Brudvig, Inorg. Chem. 46 (2007) 2193.
[98] U. Bossek, M. Saher, T. Weyhermüller, K. Weighardt, Chem. Soc. Chem. Commun. (1992) 1780.
[99] X. Jiang, H. Liu, B. Zheng, J. Zhang, Dalton Trans. (2009) 8714.
[100] M. Delroisse, A. Rabion, F. Chardac, D. Tétard, J.-B. Verlhac, L. Fraisse, J.-L. Séris, J. Chem. Soc., Chem. Commun. (1995) 949.
[101] J. Glerup, P.A. Goodson, A. Hazell, R. Hazell, D.J. Hodgson, C.J. McKenzie, K. Michelsen, U. Rychlewska, H. Toftlund, Inorg. Chem. 33 (1994) 4105.
[102] B.K. Shin, M. Kim, J. Han, Polyhedron 29 (2010) 2560.
[103] B.K. Shin, Y. Kim, M. Kim, J. Han, Polyhedron 26 (2007) 4557.
[104] G. Berggren, P. Huang, L. Eriksson, S. Styring, M.F. Anderlung, A. Thapper, Dalton Trans. 39 (2010) 11035.
[105] E.J. Larson, V.L. Pecoraro, J. Am. Chem. Soc. 113 (1991) 3810.
[106] E.J. Larson, V.L. Pecoraro, J. Am. Chem. Soc. 113 (1991) 7809.
[107] M.A. Vázquez-Fernández, M.R. Bermejo, M.I. Fernández-García, G. González-Riopedre, M.J. Rodríguez Doutón, M. Maneiro, J. Inorg. Biochem. (2011), doi:10.1016/j.jinorgbio.2011.09.002.
[108] J. Kaizer, B. Kripli, G. Speier, L. Párkányi, Polyhedron 28 (2009) 933.
[109] J. Kaizer, T. Csay, P. Kővári, G. Speier, L. Párkányi, J. Mol. Catal. A: Chem. 280 (2008) 203.
[110] V. Daier, D. Moreno, C. Duhayon, J.P. Tuchagues, S. Signorella, Eur. J. Inorg. Chem. (2010) 965.
[111] J.A.A.H. Lessa Jr., C.B. Pinheiro, L.L. Farah, M.N. Eberlin, M. Benassi, R.R. Catharino, C. Fernandes, Inorg. Chem. Commun. 10 (2007) 863.
[112] J.A.A.H. Lessa Jr., E.S. Bull, M.R. Rocha, M. Benassi, R.R. Catharino, M.N. Eberlin, A. Casellato, C.J. Noble, G.R. Hanson, G. Schenk, G.C. Silva, O.A.C. Antunes, C. Fernandes, Inorg. Chem. 48 (2009) 4569.
[113] M. Devereux, M. McCann, V. Leon, V. McKee, R.J. Ball, Polyhedron 21 (2002) 1063.

[114] J. Kaizer, G. Barath, G. Speier, M. Reglier, M. Giorgi, Inorg. Chem. Commun. 10 (2007) 292.
[115] P.K. Gonzalez, J. Zhuang, S.R. Doctrow, B. Malfroy, P.F. Benson, M.J. Menconi, M.P. Fink, J. Pharmacol. Exp. Ther. 275 (1995) 798.
[116] W. Park, D. Lim, Bioorg. Med. Chem. Lett. 19 (2009) 614.
[117] S.R. Doctrow, K. Huffman, C.B. Marcus, C. Tocco, E. Malfroy, C.A. Adinolfi, H. Kruk, K. Baker, N. Lazarowych, J. Mascarenhas, B. Malfroy, J. Med. Chem. 45 (2002) 4549.
[118] Y. Watanabe, A. Namba, N. Umezawa, M. Kawahata, K. Yamaguchi, T. Higuchi, Chem. Commun. (2006) 4958.
[119] V. Lanza, G. Vecchio, J. Inorg. Biochem. 103 (2009) 381.
[120] D. Moreno, V. Daier, C. Palopoli, J.P. Tuchagues, S. Signorella, J. Inorg. Biochem. 104 (2010) 496.
[121] B.J. Day, Biochem. Pharmacol. 77 (2009) 285.
[122] T. Hanawa, S. Asayama, T. Watanabe, S. Owada, H. Kawakamai, J. Control. Release 135 (2009) 60.
[123] M.W. Brazier, S.R. Doctrow, C.L. Masters, S.J. Collins, Free Radic. Biol. Med. 45 (2008) 184.
[124] B.J. Day, Drug Discov. Today 9 (2004) 557.
[125] M.C. McDonald, R.E.d.V. Bianca, N.S. Wayman, A. Pinto, M.A. Sharpe, S. Cuzzocrea, P.K. Chatterjee, C. Thiemermann, Eur. J. Pharmacol. 46 (2003) 181.
[126] B.J. Day, Arch. Biochem. Biophys. 347 (1997) 256.
[127] J.I. Yang, D.G. Nocera, J. Am. Chem. Soc. 129 (2007) 8192.
[128] M. Maneiro, M.R. Bermejo, M.I. Fernández, E. Gómez-Fórneas, A.M. González-Noya, A.M. Tyryshkin, New J. Chem. 27 (2003) 727.
[129] C. Palopoli, N. Bruzzo, C. Hureau, S. Ladeira, D. Murgida, S. Signorella, Inorg. Chem. 50 (2011) 8973.